Chapter 8

Techno-Economics of Hybrid NF/FO with Thermal Desalination Plants

Abdel Nasser Mabrouk, Hassan Fath,
Mohamed Darwish and Hassan Abdulrahim

Additional information is available at the end of the chapter

http://dx.doi.org/10.5772/60207

Abstract

Hybrid desalination technology is defined as any combination of thermal and membrane processes in seawater desalination systems. So far, the two technologies have evolved rather independently with some degree of competition. Traditionally, in co-generation market applications, thermal desalination has succeeded in establishing a stronghold where large capacities are needed, energy costs are low, and seawater quality is challenging. However, in recent years, membrane systems have also succeeded in grabbing a larger share of the world seawater desalination market, mainly as a result of progress made in membrane and energy recovery technologies. Realizing the potential benefits and challenges faced by both technologies on their own, designers have been looking for ways to synergize and combine the two technologies in optimum configurations, which promise to further reduce the total cost of seawater desalination.

Several studies have been published over the past 20 years addressing the potential of integrating hybrid desalination systems. Coupling schemes worth noting for hybrid systems include RO preheating using condenser heat reject of the associated distillation unit; the use of membrane filtration upstream of MSF, MED, and RO systems; brine recirculation coupling; product blending; and the use of common intake and outfall systems. To date, commercially available hybrid desalination plants are of the simple non-integrated type. They may share common systems such as intake and outfall facilities, but otherwise they run independently at the same site. Product water from the membrane and thermal systems are usually blended to international standards on water quality. One more step ahead this chapter addresses the role of

using forward osmosis (FO) or nano-filtration (NF) as a pre-treated method to the existing thermal desalination plants. The target of this hybridization is to reduce divalent ions that cause hard scale deposition at elevated temperature. The separation of divalent ion enables the increase of the desalination process temperature greater than 110°C, which consequently increases the plant performance, increases the productivity, and reduces the chemical consumption.

Integrating the NF system with new (MSF-DBM) configuration enables to increase the TBT up to 130 °C. The new NF-MSF-DBM configuration significantly reduces the unit's input thermal energy to suit the use of (the relatively expensive) solar energy as a desalination plant driver. The desalination pilot test is built to evaluate the performance of the novel de-aeration and brine mix (MSF-DBM) configuration at high top brine temperature (TBT) using NF membrane. The capacity of the desalination pilot plant is 1.0 m^3/day of water. Comparisons between the simulation and the experimental results of the pilot unit subsystems are relatively satisfactory. The newly developed NF-MSF-DBM (de-aerator and brine mix) configuration is tested at TBT = 100 °C. The gain output ratio (GOR) is calculated as 15, which is almost twice the GOR of the traditional MSF. High GOR NF-MSF-DBM system requires lower input thermal energy, which makes the integration with (the relatively expensive) RE system as a desalination plant driver, viable option.

Simulation results showed that integrating FO to existing MSF and using brine of the last stage as a draw solution at a recovery ratio of 35% reduce the Ca+ ions in the seawater feed by 20%, which enables increasing the TBT up to 130°C safely. The simulation results show that, the production of the existing MSF plant increases by 20% as a result of working at higher temperature of TBT=130 °C. The specific operating cost (OPEX) analysis showed that up to 2.3 M$/year of chemical cost can be saved if the FO membrane is deployed to the existing MSF desalination plants in Qatar.

Keywords: Desalination, Thermal, Membrane, Hybrid, Cost

1. Introduction

1.1. Hybrid desalination concept

Hybrid technology is defined as any combination of thermal and membrane processes in seawater desalination systems. So far, the two technologies have evolved rather independently with some degree of competition. Traditionally, in co-generation market applications, thermal desalination has succeeded in establishing a stronghold where large capacities are needed, energy costs are low, and seawater quality is challenging. However, in recent years, membrane systems have also succeeded in grabbing a larger share of the world seawater desalination market, mainly as a result of the progress made in membrane and energy recovery technologies. Realizing the potential benefits and challenges faced by both

http://dx.doi.org/10.5772/60207

technologies on their own, designers have been looking for ways to synergize and combine the two technologies in optimum configurations, which promise to further reduce the total cost of seawater desalination.

Several studies have been published over the past 20 [1-14] years addressing the potential of integrating hybrid desalination systems. Coupling schemes worth noting for hybrid systems include RO preheating using condenser heat reject of the associated distillation unit; adding thermal vapour compression to MED systems; the use of membrane filtration (NF) upstream of MSF, MED, and RO systems; brine recirculation coupling; product blending; and the use of common intake and outfall systems.

To date, commercially available hybrid plants are of the simple non-integrated type. They may share common systems such as intake and outfall facilities, but otherwise they run independently at the same site. Product water of both membrane and thermal plants are usually blended to meet the international standards water quality specifications. Examples of existing hybrid plants include Jeddah, Al-Jubail, and Yanbu in Saudi Arabia. Recently, a power and water plant has been designed and built by Doosan in Fujairah (UAE). This plant produces 500 MW of net electricity to the grid and 100,000 MIGD of fresh water, 63% of which is produced by MSF with the balance produced by RO [1].

1.2. NF's role in desalination

NF, in particular, has been advocated as a pretreatment option upstream of a thermal desalination unit [2-8]. Due to small pore size and charge at the surface of the membrane, NF is known to remove divalent ions, including a fraction of scale-producing hardness and salts, allowing in principle at least a possible increase in top brine temperature and promising improved steam economy. Studies on NF-MSF pilot tests claim scale-free operation for 1,200 hours with top brine temperatures reaching 130°C, reporting an improvement in recovery from 30% for stand-alone MSF to 70% with NF [2-8]. The integration of NF –MED system is under pilot investigation by Saline Water Desalination Research Institute (SWDRI) with Sasakura (a Japanese-based consortium) [15]. Implementation of dual-stage NF has been successful evaluated at Long Beach, California [16]. From the present analysis, NF will play a crucial role in desalination, provided that the cost of NF membrane would be decreased. Efficient removal of boron has also been reported [16]. However, the reliability and economic viability of such a design need to be confirmed, considering the higher thermal and pressure load implied by the design and the additional capital, energy, and operation and maintenance costs of membrane pre-treatment components. Adding to the uncertainty are increased risks for corrosion and the long-term reliability of such a system.

1.3. FO role in desalination

The role of using forward osmosis (FO) as a pre-treated method to the existing thermal desalination MSF/MED plants is to reduce divalent ions that cause hard-scale deposition at elevated temperature. The removal of the divalent ions, such as $CaSO_4$, from the MSF feed enables to increase the desalination process temperature greater than 110°C. Consequently the

plant performance and productivity will increase. Due to the removal of the ions which cause scale deposit, the chemical additive consumption will be decreases. In the MSF process due to working at higher temperature, hard scale, such as calcium sulphate, is formed. As calcium sulphate is two orders of magnitude more soluble than calcium carbonate, the sulphate is much less likely to drop out of solution when both are present.

In the light of the recent development in the membrane filtration technologies, the cost of seawater pretreatment can be reduced if FO membranes were used with/without NF. The novel application of FO membrane for seawater filtration requires, firstly, retrofitting the FO system to the thermal desalination unit. Secondly, it also requires finding a suitable draw solution that would reduce the cost of FO pre-treatment. Fortunately, the current FO membranes exhibit high water permeability and rejection rate, which make them an ideal solution for seawater pretreatment [17]. A novel hybrid FO-thermal desalination system to remove scale deposit elements from seawater to the thermal units, is presented [17-18]. The performance of the thermal evaporator was evaluated after introducing the FO pretreatment. The scale deposition on the thermal unit was estimated by using special software to predict the precipitation on inversely soluble metal ions on the heat exchangers [17-18].

1.4. Objective

This chapter addresses the role of using FO or NF as a pre-treated method to the existing thermal desalination plants. The target of this hybridization is to reduce divalent ions that cause hard-scale deposition at elevated temperature. The separation of divalent ion enables the increase of the desalination process temperature greater than 110°C, which consequently increases plant performance and productivity, as well as reduces the chemical consumption.

2. Process description

2.1. MSF-RO hybrid

The simple type refers to co-located thermal and membrane systems that may share some common systems on site. This in turn facilitate blended to product water specifications, but otherwise are running independently. Examples include the Fujairah plant and three Saudi plants in Jeddah, Al-Jubail, and Yanbu. The Fujairah plant [1], representing a simple hybrid type, was constructed by Doosan Heavy Industries and is currently considered the largest existing hybrid type. The plant is rated at 100 MIGD, of which 63% are produced by MSF and 37% by RO. Featuring a combined cycle system, it also generates 500 MW to the grid. The thermal part of the plant includes five MSF evaporators rated at 12.5 MIGD each, with a top brine temperature of 110◦C. The membrane part includes two RO passes, using a conventional pretreatment system and energy recovery devices of the Pelton type. A specification of 200 PPM as the maximum water product salinity was met by the design.

Another option of a hybrid type is to improve the membrane performance. This type includes the integration of hybrid membrane and thermal systems, with the aim of improving mem-

http://dx.doi.org/10.5772/60207

brane recovery by preheating the RO feed using heat reject from the thermal unit as shown in Figure (1). Higher temperatures are known to improve membrane flux, mainly as a result of reduced viscosity. Several investigators examined the effects of preheating in pilot tests, and about 3% of recovery improvement is reported per degree Celsius [19]. This should, however, be weighed against potential negative effects of high temperatures on membrane performance, in particular compaction damage. Membrane manufacturers have traditionally set an upper temperature limit of 40◦C for the use of their membranes, and it is not clear how close to this limit operation should be, in order to optimize life-cycle membrane performance and costs. The measure is particularly useful in winter when seawater temperatures are reduced.

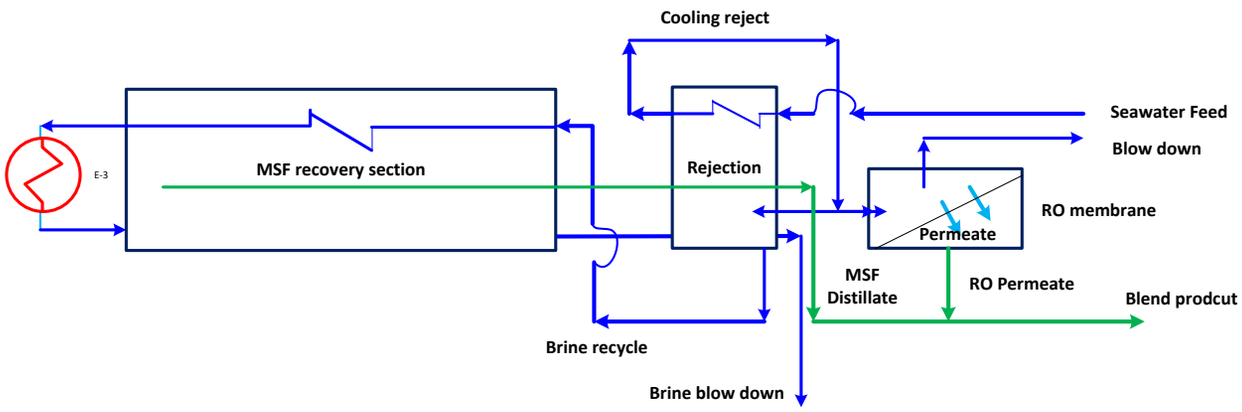

Figure 1. Process flow diagram of hybrid RO-MSF process

Preheating the Fujairah RO feed in winter is an example of integrated hybrid operation, representing type 2. A 10°C increase from 23°C to 33°C for an RO unit equivalent in capacity to the Fujairah plant would increase recovery by about 30% and, therefore, reduce feed pressure requirements. This preheating feature could then be made to good use in the winter when seawater temperatures in the Gulf drop by 15–20°C.

2.2. NF-MSF process

This type includes the integration of hybrid membrane and thermal systems with the objective of improving the gain output ratio (GOR) and steam economy of the thermal system (see Figure 2). The GOR is a function of the available temperature range and can, therefore, be improved by increasing the top brine temperature (TBT). Traditionally, the top brine temperature is limited to 110 °C for MSF and is limited to 65◦C for MED. This practice, in addition to chemical dosing and mechanical cleaning, is necessary to minimize scale deposition on heat transfer surfaces. Some investigators have advocated the use of NF membrane upstream of the thermal system as a pretreatment step to reduce scaling hardness and additionally some salt. This would, in principle, allow operation at higher temperatures, without increased scaling. SWCC investigators have tested a hybrid NF/MSF pilot unit running at a top brine temperature of 130°C for a period of 1,200 hours and reported a doubling in the recovery with no observed scale formation [10].

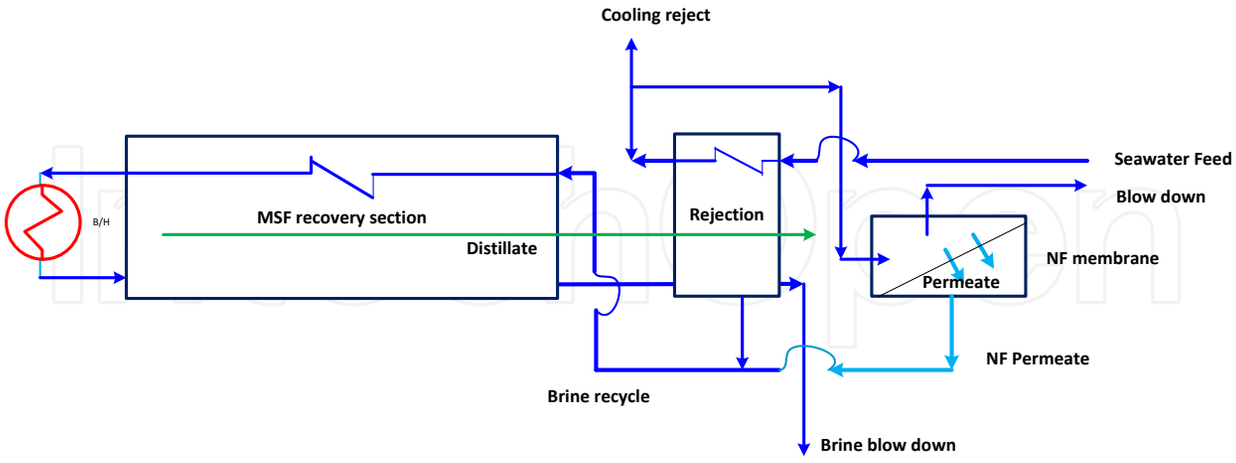

Figure 2. Process flow diagram of hybrid NF-MSF process

2.3. FO-MSF

Figure 3 shows hybrid FO-multi stage flash (FO-MSF) system for high TBT MSF. In this type of hybrid system, the brine reject from the thermal desalination process will be considered as a draw solution, while the cooling seawater exiting from the MSF heat rejection section will be used as a feed solution. Permeate water will transport across the FO membrane from the feed to the draw solution side while monovalent and multivalent ions are rejected by the FO membrane. After leaving the FO membrane, the concentrated seawater is dumped back to the sea. Simultaneously, the diluted draw solution from the FO process is circulated to the MSF recovery section. Inside the MSF plant, fresh water is extracted from the draw solution by evaporation and is condensed in the consecutive MSF chambers. The distilled water is collected at the last stage and directed to the distilled tank. The un-flashed brine through MSF stages (brine pool) is collected in the last stage of MSF evaporator at high salinity and then is directed to the FO as a draw solution.

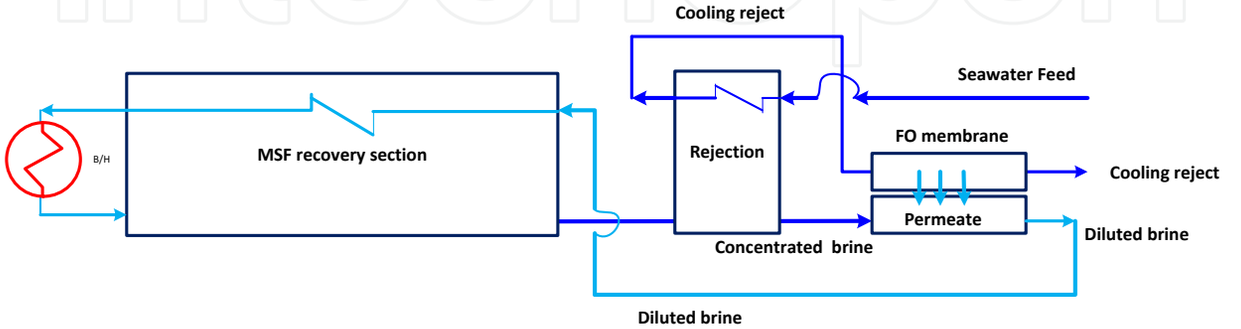

Figure 3. Process flow diagram of hybrid FO-MSF process

http://dx.doi.org/10.5772/60207

2.4. FO-MED

Figure 4 shows the hybrid FO-multi effect distillation (FO-MED) system for high TBT MED. In this type of hybrid system, the brine reject from the last effect will be considered as a draw solution stream, while the condenser cooling seawater will be used as a feed solution stream. Permeate water will transport across the FO membrane from the feed to the draw solution side while monovalent and multivalent ions are rejected by the FO membrane. After leaving the FO membrane, the concentrated seawater is dumped back to the sea water. Simultaneously, the diluted draw solution from the FO process is circulated to the MED evaporator as a makeup feed. Inside the MED evaporator, fresh water is extracted from the draw solution by evaporation and is condensed in the consecutive MED effect. The distilled water is collected at the last effect and is directed to the distilled tank. The brine (un-evaporated) through MED effect is collected in the last effect at a high salinity is directed to the FO again as a draw solution.

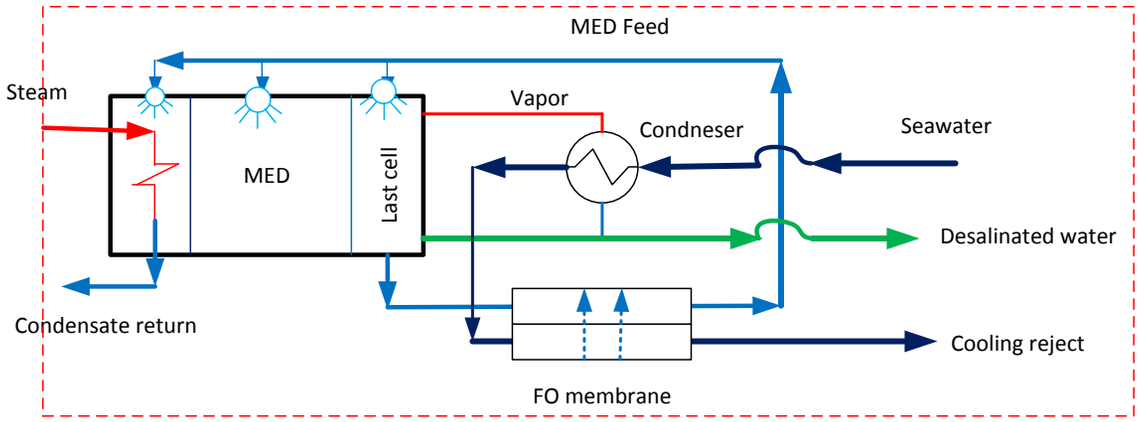

Figure 4. Process flow diagram of hybrid FO-MED process

3. Methodology

3.1. Mathematical model development of NF

Figure 5 illustrates the input and output parameters used for the mass and energy balance equations of the NF membrane [13-14].

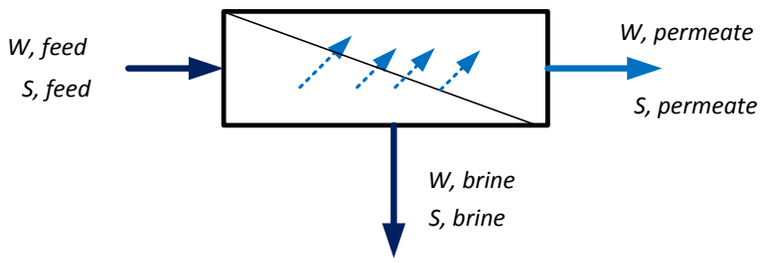

Figure 5. Schematic diagram of the NF membrane streams

Mass balance is written as follows:

$$W_{f,j} = W_{p,j} + W_{b,j} \tag{1}$$

$$S_{f,j} = S_{p,j} + S_{b,j} \tag{2}$$

The following relation defines the rate of water passage through a semipermeable membrane [14]:

$$W_{p,j} = (\Delta P_j - \sigma \Delta \pi_j) \times K_w \times A_j \times TCF \times FF \times \rho_{p,j} \tag{3}$$

$$\Delta P_j = \overline{P}_j - P_{p,j} \tag{4}$$

$$\Delta \pi_j = \bar{\pi}_j - \pi_{p,j} \tag{5}$$

$$\bar{P}_j = 0.5(P_{f,j} + P_{b,j}) \tag{6}$$

As the seawater salt concentrations ratio is almost constant, an approximation for value in kPa can be given as [13]:

$$\pi = 6.895 \times \frac{38.5 \times C_{fbNaCl} \times (T + 273)}{1000 + C_{fbNaCl}} \tag{7}$$

$$C_{fbNaCl} = 0.934348 \times C_{fb} - 0.54169 \tag{8}$$

The rate of salt flow through the membrane is defined as:

$$S_{p,j} = (C_{m,j} - C_{p,j}) \times K_s \times A_j \times TCF + (1 - \sigma) \times J_{v,j} \times \bar{C} \times K_s \times A_j \times TCF \tag{9}$$

$$J_{v,j} = (\Delta P_j - \sigma \Delta \pi_j) \times K_w \times FF \times TCF \left(m/s\right) \tag{10}$$

Where, the temperature factor correction (TCF) is calculated using the following equations [14]:

$$TCF = e^{8.859 \times \frac{T-25}{T+273}}, \text{ for } T \geq 25°\text{C} \tag{11}$$

$$TCF = e^{11.678 \times \frac{T-25}{T+273}}, \text{ for } T \geq 25°\text{C} \tag{12}$$

$$C_{p,j} = S_{p,j} \times \rho_{p,j} / (S_{p,j} + W_{p,j}) \tag{13}$$

http://dx.doi.org/10.5772/60207

A material balance within the mass transfer boundary layer near the membrane wall between the solute carried to the membrane by convection and the solute carried away by diffusion yields an expression that quantifies concentration polarization:

$$\varphi = \frac{C_m - C_p}{C_b - C_p} = e^{J_w/k} \tag{14}$$

The Umm-Lujj NF-RO plant [20] is considered as a case study to verify the mathematical model of the NF membrane equation (1-14), as well as to estimate the permeate constant Kw and the solute constant Ks.

This plant consists of 27 pressure vessels and six NF elements per vessel. The feed characteristic is 360 m^3/hr, the temperature is 32°C, and the salinity is 45.46 g/l. The applied feed pressure is 25 bars. The data from the Umm-Lujj plant, shown in Table (1), are used as the input data of VDS [21-25] software as shown in Figure 6.

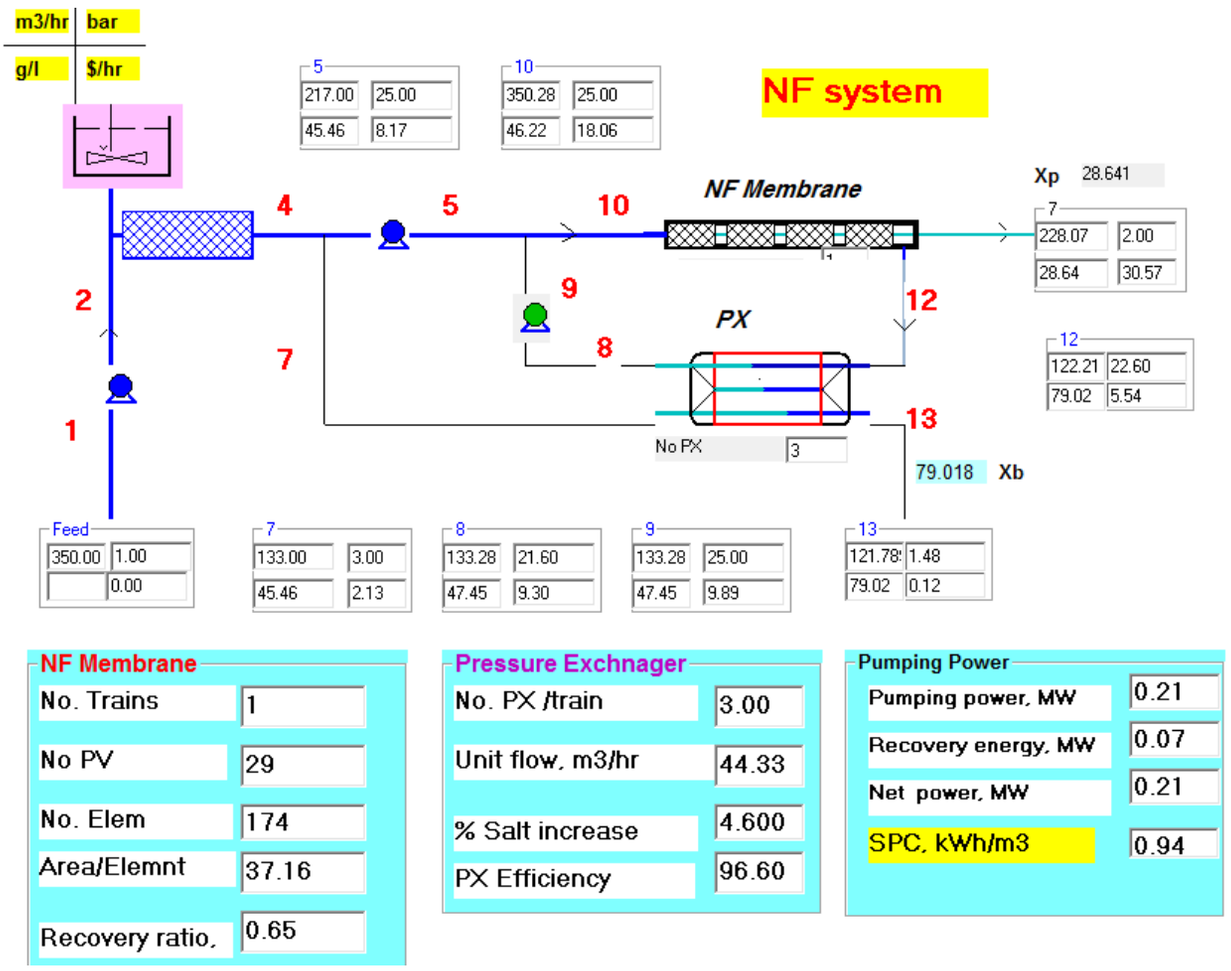

Figure 6. VDS interface of the NF system with pressure exchanger

The VDS simulates the Umm-Lujj plant of NF to estimate the permeate production and the exact value of the membrane constants Kw and Ks. After several runs, the membrane water permeability K_w of the considered NF membrane is determined as follows:

$$K_w = 5.8 \times 10^{-9}\ \mathrm{m^3/m^2.s.kPa} \tag{15}$$

The membrane salt permeability coefficient K_s is estimated as follows:

$$K_s = 9 \times 10^{-8} \tag{16}$$

Using the estimated values Kw and Ks, the VDS results are compared against the typical plant as shown in Table (1). The comparison results show a good agreement between the VDS results and the typical real plant.

Variable	VSP results	Umm-Lujj	% Error
Feed flow rate, m^3/hr, *	360	360	-
Feed salinity, TDS, g/l, *	45.46	45.46	-
Stages No.*	1	1	-
No. of pressure vessels, *	27	27	-
Feed temperature, °C, *	32	32	-
Fouling factor, *	0.95	NA	-
Feed pressure, bar, *	25	25	-
Elements No. per vessel, *	6	6	-
Permeate flow rate, m^3/hr	245	234	4.7%
Recovery ratio	0.68	0.65	4.6%
Permeate salinity, TDS, mg/l	29.11	28.26	3%

Table 1. Comparison between VDS and Umm-Lujj typical results

*Input data to the VDS

The VDS program is used to size the NF system to produce 226 m^3/hr, which represents one-third of the makeup feed, which is required for 1 MIGD MSF. The required number of pressure vessels is calculated as 29 with 174 membrane elements. The calculated system recovery ratio is 65%. The high-pressure pump is assigned by 25 bars. Three units of pressure exchangers are used to recover an electrical energy of 0.07 MW. Each unit's capacity is 44 m^3/hr, and the percentage of salt increase is only 4.6%. The net pumping power required is 0.21 MW, and the specific power consumption is 0.94 kWh/m^3.

http://dx.doi.org/10.5772/60207

3.2. Mathematical model of forward osmosis (FO)

Forward osmosis is the transport of water across a selectively permeable membrane from a region of higher water chemical potential (feed solution) to a region of lower water chemical potential (draw solution). Consequently, a less concentrated draw solution is being produced, which may be further treated to extract freshwater. Obviously, there are two key problems that must be solved to make the technology go out of the laboratory. One is continued improvement and optimization of the selectively permeable membrane, which allows passage of water but rejects most solute molecules or ions. The other is the identification of optimal osmotic agents and its corresponding recovery processes for the supply of the osmosis pressure difference, which is the driving force of the FO process. However, the FO membrane water flux is far lower than the anticipated when the membrane used is asymmetric. The primary reason for this finding is the fact that both FO are accompanied by internal concentration polarization (ICP) as shown in Figure 7.

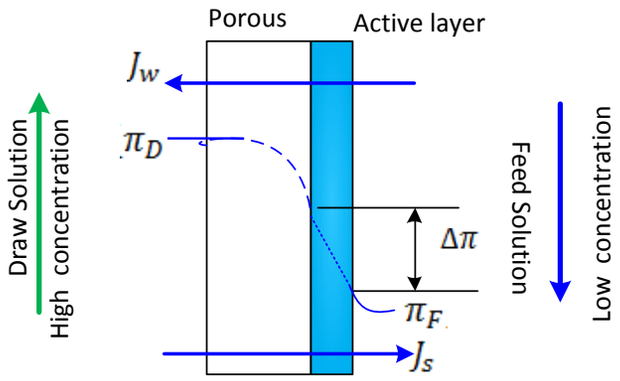

Figure 7. Concentration profile in asymmetrical FO membrane

In the work of Jung et al. [26], FO performance (permeate flux and recovery rate) of a 10 cm ×10 cm plate and frame type membrane is investigated via a numerical simulation based on the mass conservation theorem. The FO membrane orientation, flow direction of feed and draw solutions, flow rate, and solute resistivity (K) are simulated. The case of draw solution facing the active layer displays a relatively higher performance than the feed solution facing the active layer [26]. The numerical results showed that the membrane performance is much more sensitive to the physical membrane property parameter rather than the flow rate and flow direction. However, the simulation methodology does not consider fouling and reverse solute diffusion. Also, the performance of the FO in a relatively large size needs to be explored to come up with a concrete recommendation to the commercialization phase.

A simple schematic of the FO process is shown in Figure 8. The mathematical model of FO membrane is developed as shown in equations (17-26). By knowing the specifications of the FO membrane,, and the membrane area, the outlet stream can be calculated.

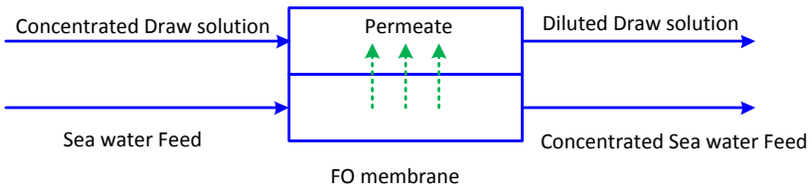

Figure 8. Schematic of the FO membrane process

$$W_{DS,outlet} - W_{DS,inlet} = W_p \tag{17}$$

$$S_{DS,out} - S_{DS,inlet} = S_p \tag{18}$$

$$W_{FS,in} - W_{FS,out} = W_p \tag{19}$$

$$S_{FS,in} - S_{FS,\,out} = S_p \tag{20}$$

$$W_p = J_w \times A \times \rho \tag{21}$$

$$S_p = J_s \times A \tag{22}$$

The general flux equation in the FO process is

$$J_w = A\left(\pi_D - \pi_F\right) \tag{23}$$

where A is the water permeability coefficient, and and denote the osmotic pressures of the draw and feed solution, respectively. The osmotic pressure can be determined by the modified Van't Hoff equation as:

$$\Delta\pi = \frac{N_{ion} R_g T \Delta C}{M_w} \tag{24}$$

where T, and indicate the ionization number of the solution, the ideal gas constant, the absolute temperature, the salt concentration difference of the solution across the membrane, and the molecular weight of the salt, respectively. For asymmetrical membrane, internal ICP occurs within the porous support as shown in Figure 7. However, when the reverse solute is considered [27], and for the case of the draw solution facing the porous layer, the water flux and solute flux are:

$$J_w = A\left(\frac{\pi_D exp\left(-\frac{J_w S}{D}\right) - \pi_F exp\left(\frac{J_w}{k}\right)}{1 + \frac{B}{J_w}\left[exp\left(\frac{J_w}{k}\right) - exp\left(-\frac{J_w S}{D}\right)\right]}\right) \tag{25}$$

$$J_s = B\left(\frac{C_D exp\left(-\frac{J_w S}{D}\right) - C_F exp\left(\frac{J_w}{k}\right)}{1 + \frac{B}{J_w}\left[exp\left(\frac{J_w}{k}\right) - exp\left(-\frac{J_w S}{D}\right)\right]}\right) \tag{26}$$

http://dx.doi.org/10.5772/60207

where B is the salt permeability coefficient.

The water flux and reverse solute equations are difficult to solve analytically because these equations are dependent on water flux and solute passage including in concentration polarization terms. Thus, using a program to solve these equations will be presented.

The FO is still facing many challenges such as internal concentration polarization, which requires breakthrough in the molecular design of high-performance FO membrane. On the other hand, development of draw solution with low cost and low energy consumption required for recovery is urgently needed. To mitigate ICP, the FO membranes must have characteristics of high permeability and hydrophobicity with a small structure parameter, while the preferred draw solutes must have diffusion coefficient, reasonable molecular size, and low viscosity [52].

The VDS Software interface is developed to consider a case study as shown in Figure 9. As shown in Figure 9, the specified feed solution of (1680 t/h and 45 g/l) is pumped to the FO membrane against a draw solution (NaCl) (1200 t/h and 90 g/l). Three elements per vessel are arranged. Two pressure vessels are placed in parallel. The VDS simulated the case, and the results are presented in the same interface as shown in Figure 9. The diluted flow rate is calculated as 1744 t/h and 64.34 g/l, while the concentrated feed solution is calculated as 1135.8 t/h and 66.46 g/l. Based on these calculations, the system recovery ratio is calculated as 45%, and the specific power consumption is calculated as 0.55 kWh/m^3. So far, the effect of concentration polarization is not considered yet.

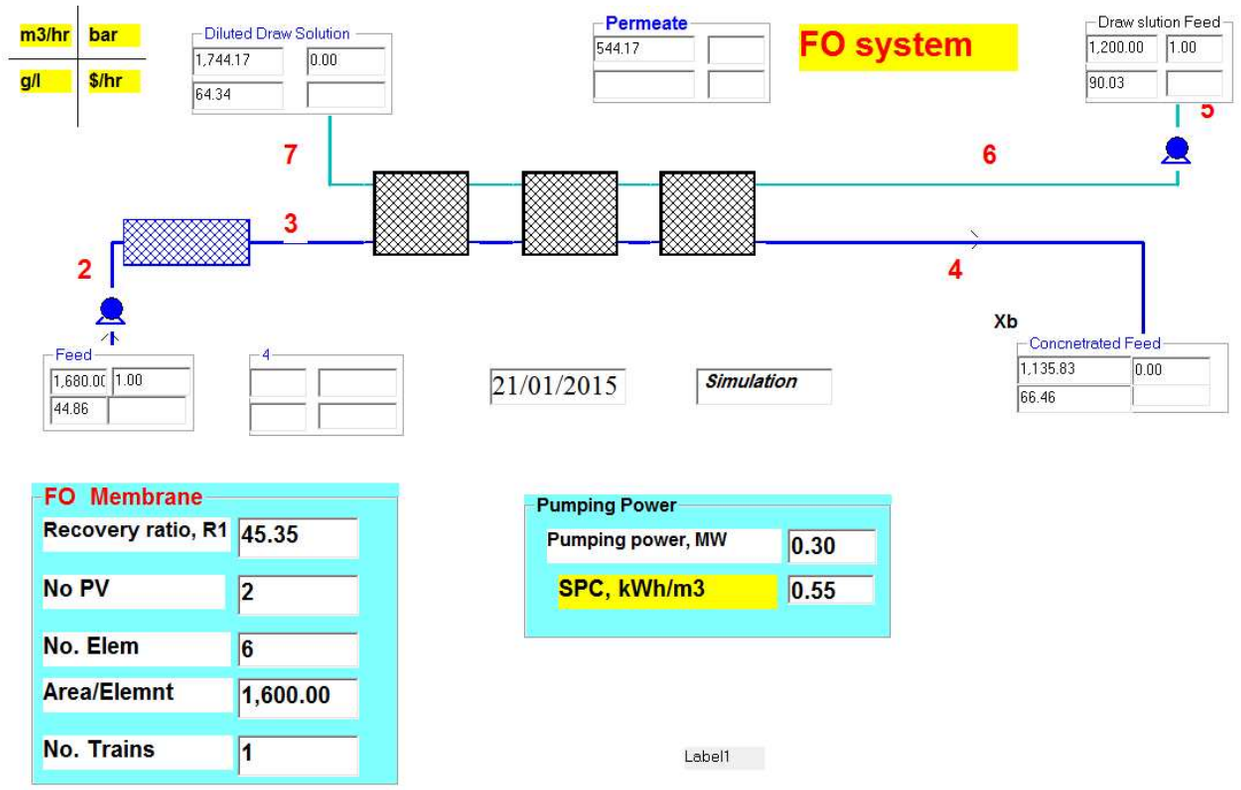

Figure 9. Interface of VDS software for FO process

4. Technoeconomic analysis

4.1. NF-MSF

The first MSF of 0.5 MGD per unit evaporator was built in 1957 in Kuwait using the once through MSF-OT configuration by the Westinghouse Company [28]. The design was modified according to the recommendation of the client, the Ministry of Electricity and Water, in Kuwait and of engineers for reliable operation. For some time, the market was dominated by the once through (MSF-OT) due its simplicity and high thermodynamic efficiency. However, due to high oxygen and CO_2 gas liberation in addition to large amount of feed water to be pre-treated, the market was forced to shift to the brine recirculation configuration (MSF-BR). The first 19-stage 1 MGD MSF-BR plant was built by Weir Company in 1959 in Kuwait [28]. The developed specifications led to more reliable, easy-to-operate-and-maintain, and longer life units. Now, the MSF evaporator production capacity was increased dramatically through the years to reach 20 MGD in UAE, and designs of 25-30 MIGD are available. The disadvantage of the MSF-BR system is the higher brine concentration, which increases the potential for having scale deposits on the heat transfer surfaces and for the liquid boiling point elevation (BPE), thus penalizing the coefficient of heat transfer and the available condensing temperature difference, respectively.

Increasing the MSF unit production (for both new designs and operating units) can be carried out either by: i) increasing the re-circulating brine flow rate, or ii) increasing the flashing range. Increasing the re-circulating brine flow rate is limited, however, by the available pump capacity and the chamber load (flashing brine flow velocity). Increasing the flashing range (TBT–BBT) can be carried out by increasing the top brine temperature (TBT), with hard-scale solution, or reducing the bottom brine temperature (BBT), with lower heat sink temperature (naturally in fall/winter/spring or utilizing deep intake or cooling towers). Increasing TBT is the parameter addressed in this paper.

At high TBT, scale deposits of high seawater brine concentration present a real problem in MSF plants, as they directly affect the heat transfer rates on the heating surface. The main scale-forming constituents are calcium (Ca^{++}), magnesium (Mg^{++}), bicarbonate ($HCO3^{-}$), and sulphate ($SO4^{--}$) ions. On heating, bicarbonate decomposes into carbonate $CO3^{-}$, which reacts with Ca^{++} forming calcium carbonate (CaCO3) that precipitates on the heat transfer surface (if saturation limits are exceeded). At high temperature, magnesium hydroxide (MgOH) will also be formed. At higher temperature of >120°C, non-alkaline calcium sulphate (CaSO4) precipitates if saturation limits are also exceeded, due to inverse solubility. Formation of alkaline scale (CaCO3 and MgOH) can be controlled by lowering the pH (acid additives) or by anti-scalant. Non-alkaline (hard) scale (such as CaSO4) is only controlled nowadays by limiting the TBT below 120°C.

Scale deposits have a direct influence on the thermal units' performance and water cost. Sulphate scales are a result of the direct crystallization of anhydrite (CaSO4), hemihydrate (CaSO4 0.5H2O), or gypsum (CaSO4 2H2O) from seawater once their solubility limits are exceeded as shown Fig. 10 [29]. Most of the deposited calcium sulphate found in seawater

http://dx.doi.org/10.5772/60207

desalination plants is in the form of hemi-hydrate. The sulphate minerals are insoluble in common chemicals, and their development inside a distiller should be avoided by all means.

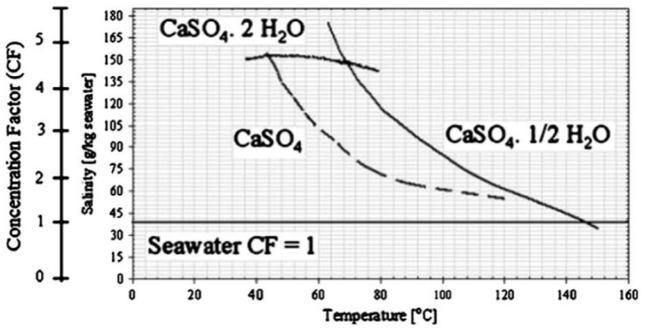

Figure 10. Phase diagram of CaSO4

Increasing the TBT with hard-scale solution can be carried out by: i) introducing high-temperature anti-scalant, and ii) reducing hard-scale ions to avoid it from reaching the saturation conditions. The first is not yet available through the use of nano-filtration (NF) membrane system for make-up feed water pretreatment.

The application of NF in seawater desalination has gained significant attention in the desalination industry due to the selective removal of divalent ions. The SWCC R&D team [30-32] carried out extensive experiments on an MSF test pilot unit with NF as the pretreatment. NF pressure was 24 bars, and its recovery ratio ranged from 60% to 65%. The total concentration of the sulphate and calcium ions of the brine recycle was at a TBT of 130°C, and the makeup entirely formed from NF permeate was below the solubility limits. This result indicated the possibility of operating the MSF plant safely and without any scaling problem at TBT equal to or higher than 130°C. However, many questions on the adding of capital cost which might result in saving in operational cost still need clear answers.

The NF was originally applied to reject electrolytes and obtain ultra-pure water with high volume flux at low operating pressure, as most membranes have either positive or negative charge due to their compositions [33]. The NF membrane possesses a molecular weight cut-off of about hundreds to a few thousands, which is intermediate between reverse osmosis (RO) membranes and ultra-filtration (UF). The pore radii and fixed charge density of practical membranes were evaluated from permeation experiments of different neutral solutes of sodium chloride. The pore radii of these NF membranes were estimated to range from 0.4 to 0.8 nm [33].

The flexible and powerful tool ''Visual Design and Simulation program (VDS)'' is used to perform process and techno-economical calculations. VDS was developed for the design and simulation of different types and configurations of the desalination processes [21-25]. Typical desalination processes are simulated to show the wide scope and high capability of the developed package. The description of the VDS software and discussions on how to access and handle the package are presented in [21-25]. In this work, the scope of the VDS program will be extended to develop and build up an NF system and a new MSF configuration model. The NF system's mathematical model will be verified using typical NF-RO plant data.

Table (2) shows the CAPEX cost analysis of the NF system, which produces 226 m^3/hr. The direct costs of the purchased equipment (membrane section, filters, pumps, valves, and piping) are included. The indirect costs of the building structure, engineering, and project development are also included. The intake cost is not included and is assumed to be included in the MSF CAPEX cost. The levelized cost is calculated (based on the 7% interest rate and 15 year life span) as 0.0775 $/$m^3$ of the NF permeate as shown in column three of Table (2).

Items	Cost, $	Specific cost, $/$m^3$
Direct cost		
PV, pass 1	26,100.00	0.001510285
Element, NF	87,000.00	0.005034285
Pumps	118,026.20	0.006829626
PX/turbine	115,359.61	0.006675323
Piping and valves	188,939.88	0.010933071
Filters	249,015.74	0.014409381
Others, building, start-up	258,803.85	0.014975773
Subtotal	1,043,245.28	0.060367744
Indirect cost		
Engineering design	131,455.62	0.007606724
Financial	164,319.52	0.009508405
Sub-total	295,775.14	0.017115129
TCI	1,339,020.42	0.077482874

Table 2. CAPEX cost analysis of the NF system [14]

Table (3) shows the operational cost of the NF system, which includes labor, O&M, NF membrane replacement, electricity, and chemicals. The analysis showed that the cost of electricity represents the biggest chunk of the total OPEX, and the specific operational cost is 0.0566 $/$m^3$ of the NF permeate. From both Table (2) and Table (3), the calculated unit permeate cost is 0.134 $/$m^3$.

Figure 11 shows the interface of the existing 5,000 m^3/day MSF-BR desalination plant at TBT=110°C [14]. The evaporator consists of 20 stages – 17 for the heat recovery section and 3 stages for the heat rejection section. The extracted steam from the power side is directed to the brine heater as a heat source. Sea water flows through the tubes of the heat rejection section condensers as a coolant. Part of this coolant outlet is used as a make-up, and the remaining coolant is rejected back to the sea. The make-up is directed to the de-aerator, and pretreatment chemicals are added, then mixed with a portion of the last-stage brine. The circulation pump circulates the diluted mixed brine to the condensers of the heat recovery section. The tube

http://dx.doi.org/10.5772/60207

Items	Cost, $/year	Cost, $/m³
Labor	21,909.27	0.011546899
Maintenance	16,431.95	0.008660173
Insurance	6,572.78	0.003464069
Membrane replacement	1,305.00	0.000687777
Electricity	34,740.04	0.018309132
Chemicals	26,401.62	0.013914513
Total	107,360.66	0.056582563

Table 3. OPEX cost analysis of the NF system [14]

materials used in this plant are CuNi 90/10 for the brine heater and heat recovery section and CuNi 70/30 for the heat rejection section. The evaporator length is 29 m, the width is 7 m, and the height is 2.5 m. The design conditions are 27°C for seawater, and the brine velocity inside the tube is 2 m/s. The working pressure of the de-aerator is 0.055 bars, which is lower than the make-up saturation temperature of 38°C.

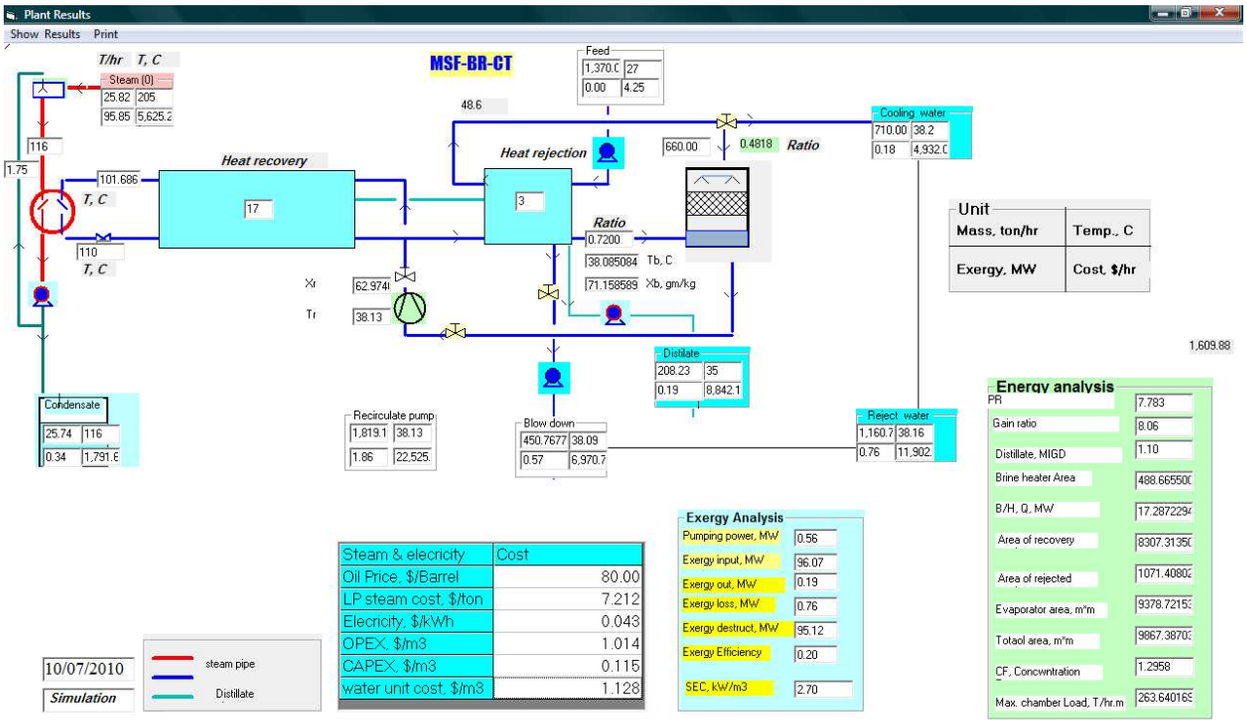

Figure 11. Interface of the existing MSF-BR desalination plant at TBT=110 C [14]

Figure 12 shows the interface the MSF-BR with the NF system, which allows increasing the TBT to 130°C. The NF system treats one-third of the make-up. The feed of the NF system is

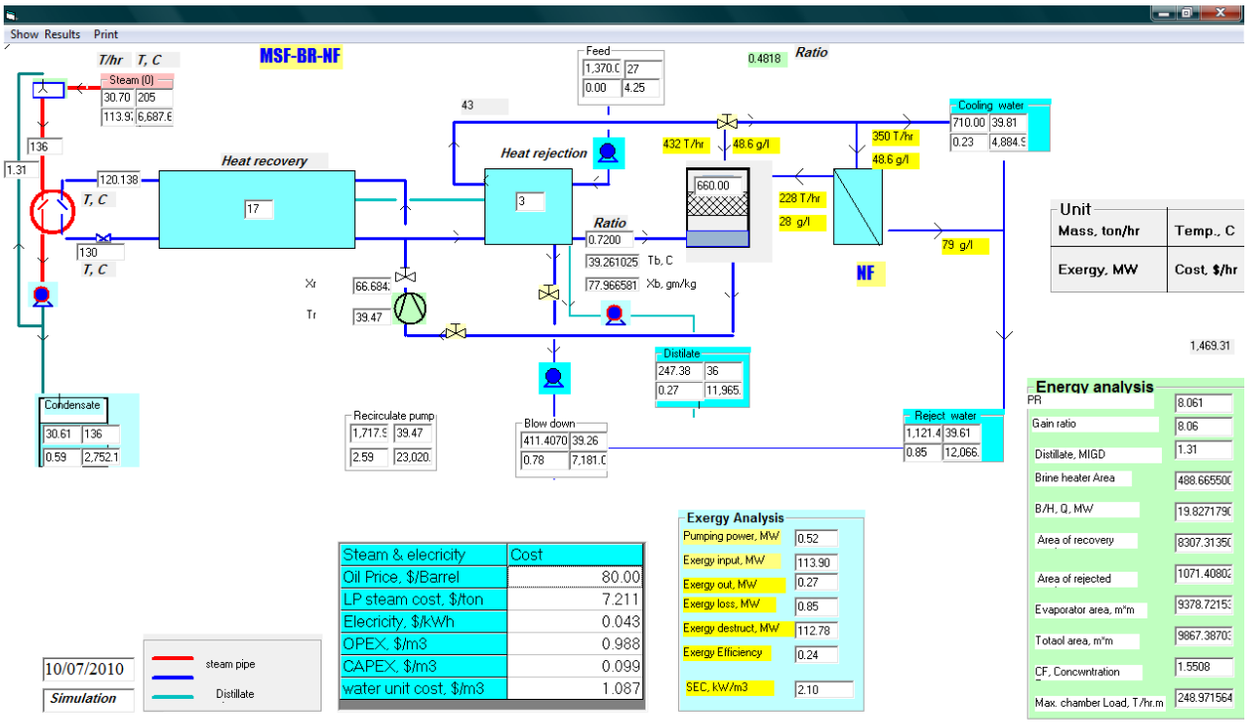

Figure 12. Interface of the NF-MSF-BR desalination plant [14]

extracted from the cooling reject stream (48 g/l) as shown in Figure (5). The NF permeate is mixed with the remaining make-up and directed to the de-aerator. The mixed make-up of low salinity of 43 g/l (15 % les) flows to the last stage of the heat rejection section. Due to the increase in the TBT from 110°C to 130°C, the distillate production increases by 19%. There is no increase of the GOR, as the heating steam increased also by 19%.

Table (4) shows that the CAPEX of the NF-MSF-BR system is 65.5% higher than that for the conventional MSF. Table (5) shows that the operating cost of the NF-MSF-BR system also increased by 22.4% higher than that for the conventional MSF.

CAPEX, 1 MIGD	**Conventional**	**NF-MSF**	**% diff**
Item	COST, US$	COST, US$	
Evaporator	1,040,551.34	1,040,551.344	-
Pumps	306,223.35	306,223.350	-
Pipes, valves, I&C	302666.77	302,666.770	-
Intake	394560	394,560.000	-
NF system	-	1,339,020.42	
Total	2,044,001.46	3,383,021.88	65.5%

Table 4. CAPEX analysis of MSF and NF-MSF-BR [14]

http://dx.doi.org/10.5772/60207

Items	MSF-BR	MSF-BR-NF	% diff
LP steam cost	186.23	221.4	18.89%
Electricity	23.8	23.8	-
Chemicals	0.48	0.48	-
Total	210.92	244.21	15.78%
NF (OPEX)		13.61753678	
Total	210.92	257.8275368	22.24%

Table 5. OPEX analysis of MSF and NF-MSF-BR [14]

Table (6) shows that the levelized CAPEX cost of MSF-BR at TBT=130°C is 16% lower than that for the conventional MSF at TBT=110°C. This is due to the increase in distillate production of 19%. Also, due to the increase in the productivity, the specific OPEX reduced by 2.5%. However, due to adding the NF system, the levelized OPEX of NF-MSF at TBT=130°C is 2.65% higher, while the specific CAPEX of NF-MSF is 28.7% higher than that for the conventional MSF.

The unit product cost of NF-MSF is 5.4% higher than that of the MSF plant. The analysis of these CAPEX and OPEX results shows that the OPEX cost has significant effect on the total unit water cost. This can be concluded that adding the NF system to an existing MSF plant (just to increase the production) is not enough to reduce the unit product cost.

	MSF-BR	MSF-BR (TBT=130°C)	% diff
Interest rate	0.07	0.07	
Life span	20.00	20.00	
Amortization factor	0.09	0.09	
Annual investment	192,468.70	192,468.70	
Hourly production	208.07	247.21	18.81%
Hourly investment	24.41	24.41	
Specific CAPEX, MSF	0.12	0.10	-15.83%
Specific OPEX, MSF	1.01	0.99	-2.50%
NF			
NF, specific OPEX		0.05	
NF, specific CAPEX		0.05	
MSF-NF, specific CAPEX	0.12	0.15	28.68%
MSF-NF, specific OPEX	1.01	1.04	2.65%
Total water unit cost	1.13	1.19	5.35%

Table 6. Levelized cost of MSF and NF-MSF-BR [14]

A modified MSF-DM configuration has been proposed as shown in Figure 13. In this MSF-DM configuration, the heat rejection section is removed, and the bottom part of the de-aerator is utilized as a mixer where part of the last stage brine is mixed with de-aerated make-up. The new configuration is half-way between brine recirculation MSF-BR and once through MSF-OT and will benefit from both techniques and overcome the limitation encountered through operation. The GOR of the MSF-DM configuration at TBT=110°C could be as high as 12.

The MSF-DM design configuration is targeting high MSF GOR to be adopted in solar energy applications (high GOR is also needed, as the cost of energy is increasing). As the capital cost in solar energy systems is expensive, it will be cost-effective to develop high-performance MSF to reduce the CAPEX of the solar energy systems. A high-performance MSF system requires a combination of more evaporating stages, and more heat transfer surface area sequentially increases the MSF CAPEX. The increase in the MSF CAPEX could be balanced by reducing the MSF OPEX, and accordingly, CAPEX reduction of the solar energy system will be the main contribution to the developed system.

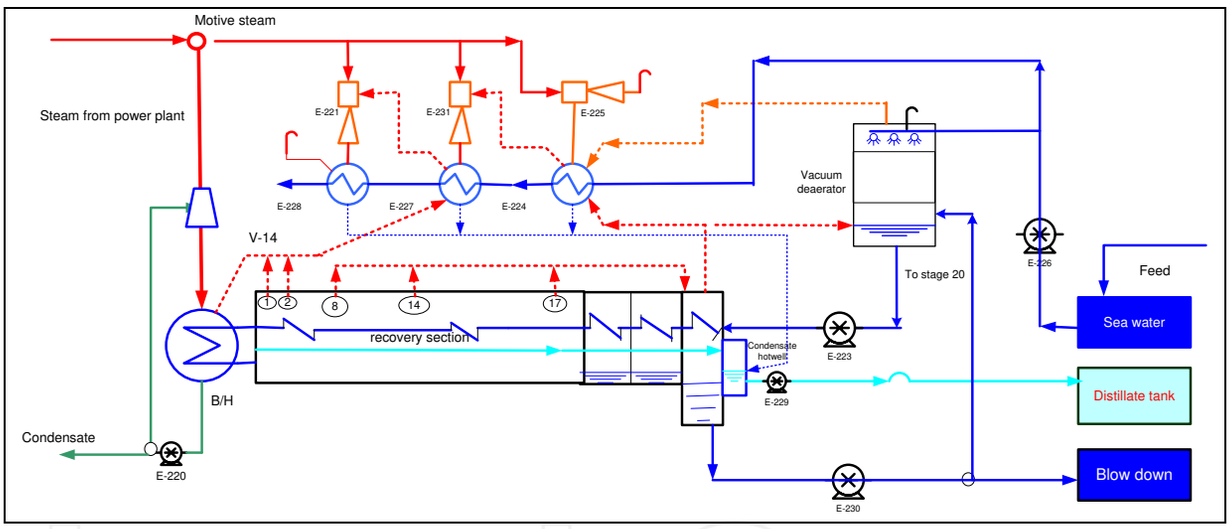

Figure 13. The interface of the new MSF-DM for desalination plant [14]

Figure 14 shows the configuration of NF with the newly developed de-aeration brine mix NF-MSF-DM system to reduce the operational cost (OPEX). NF enables increasing the TBT to 130°C, while the MSF-DM enables increasing the GOR. As shown in Figure 14, the stage number of MSF-DM increased to 35, which is 75% higher than that of the conventional MSF-BR. The 61.5% of the last-stage brine is mixed with the de-aerated make-up flow of 675 m^3/hr. The make-up is diluted from 48 g/l to 43 g/l using NF system permeate of TDS=28 g/l. This mixed is directed to the MSF condensers at 32.8°C, which is 15% lower than that for the conventional MSF (38°C). This lower temperature of coolant enhances the heat transfer process (condensation). However, the reducing cooling water reduces the LMTD across condenser compared with that of the conventional one. This explains why the heating surface area of MSF-DM was increased by 72%. One feature of increasing the heat transfer area of the heat

http://dx.doi.org/10.5772/60207

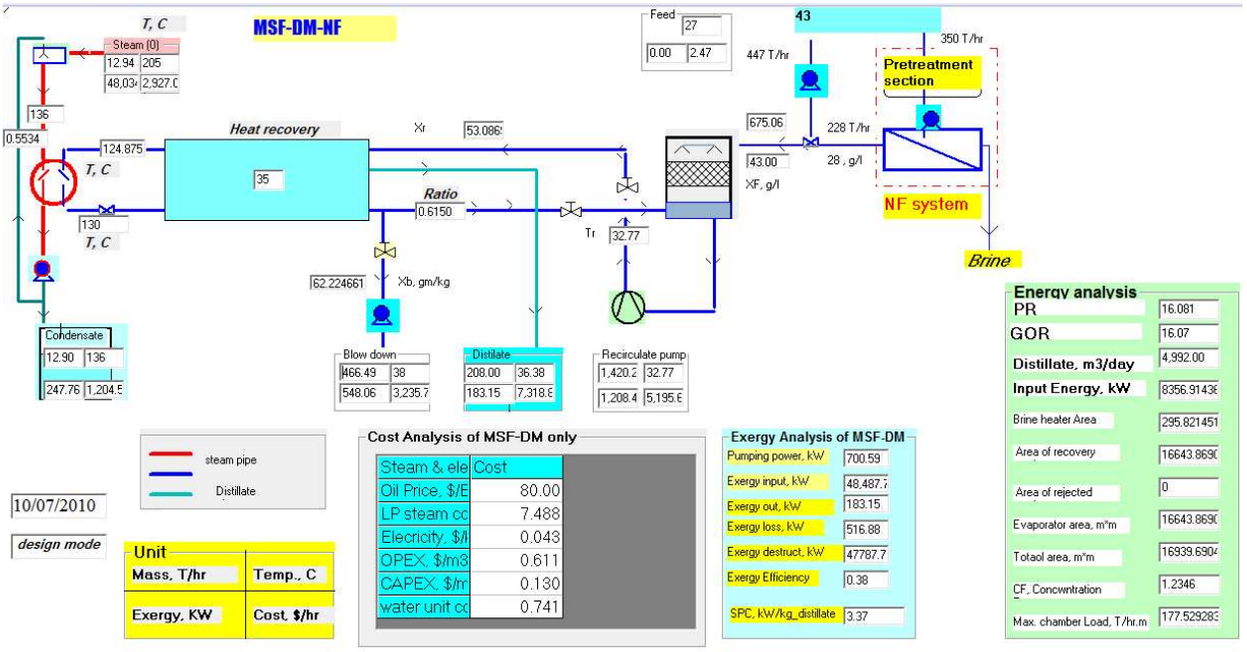

Figure 14. NF-MSF-DM configuration

recovery section is reducing the temperature difference across the brine heater, which sequentially increases the brine heater surface area. Increasing the heat transfer area of the heat recovery section increases the recovered energy, thus minimizing the external source of heating. Reducing the source of heating (steam) for fixed capacity will increase the GOR. The process calculations show that the GOR is 100% higher than that of MSF-BR (see Table (7)). This means that steam consumption is reduced by 100 %.

Table (7) shows the process calculation of MSF-DM at TBT=130°C compared with the conventional MSF at TBT=110°C. The GOR of MSF-DM-NF is twice of the conventional MSF; however, the heat transfer area is increased by 72%. Table (7) and Figure 14 show that the intake seawater of MSF-DM is 42% lower than that of MSF-BR. This, in turn, would reduce the seawater supply pump capacity, as well as the intake civil work. One feature of MSF-DM, the make is the same value of the conventional, which leads to having the same chemical cost of treatment and same manufacturing cost of de-aeration.

Table (7) shows that the specific power consumption of MSF-DM is 27% higher than that of MSF-BR. This is because of the increase of the friction loss due to the increase of the stage number by 75%. The evaporator length is increased by 142% in the case of MSF-DM; the evaporator width is decreased by 2%, while height is increased by 7% as shown in Table (7).

The purchased equipment cost (PEC) of these components is estimated based on recent market prices. In cases when data about the real installation cost of the desalination plant are scarce, the PEC of the individual components could be calculated based on cost relations. These relations of estimating the capital and operating costs of the components, such as pumps, valves, piping, and instrumentations are presented in [14].

	MSF-BR	NF-MSF-DM	% diff
Ton/hr	208	208	0%
TBT, C	110	130	18 %
Sea water flow rate, m^3/hr	1370	797	-42 %
Make-up, m^3/hr	660	675	2%
Sea salinity, g/l	48.60	48.6	0%
Recycle ratio	0.72	0.615	-15%
Recycle salinity, g/l	62.90	60	-5%
Blow down salinity, g/l	70.00	70	0%
No. of stages	20.00	35	75%
Heat transfer area, m^2	9,868	16,940	72%
Tube length, m	7.45	8	7%
Tube diameter, m	19.05	17	-11%
GOR	8	16	100%
Velocity, m/s	1.98	1.91	-4%
SPC, kWh/m^3	2.70	3.42	27%
Evaporator length, m	29.30	70.9	142%
Evaporator height	2.50	2.44	-2%
Evaporator width, m	7.45	8	7%

Table 7. Process calculation of MSF and MSF-DM [14]

A detailed cost breakdown is shown in Table (8). The evaporator (shell and tubes, de-aerator) cost of MSF-DM is 47% higher due to the increase in the heat surface area by 75% as shown in Table (7). Evaporator manufacturing cost, including the labor cost, of MSF-DM is 52% higher than that of MSF-BR. The costs of pumps, piping, valves, and I&C control of MSF-DM are lower than that of the conventional system due to the removal of the heat rejection section. The cost analysis shows that the intake construction cost of MSF-DM is 42% lower than that of the conventional one due to lower seawater flow rate. So the increase of MSF-DM evaporator cost is partially compensated by the cost reduction in auxiliaries and intake cost. The total capital cost (CAPEX) of the proposed configuration, MSF-DM, is 6% higher than that of the conventional MSF-BR. However, the total CAPEX cost of the NF-MSF-DM system is 71% higher than that of the conventional MSF. The main increase in CAPEX is contributed to the additional NF system.

Table (9) shows the OPEX items for both the conventional MSF-BR and the MSF-DM configurations. The cost of the steam and electricity is calculated based on an average of 80 $/barrel oil price and the recent purchase cost of power generation cycle [14]. The cost of the low-pressure steam is directed to the desalination plant, and the steam utilized for power generation is allocated based on exergy analysis [14]. Using levelization method through 20 years and 7%, the specific cost of low pressure steam is calculated as 7.5 $/$m^3$ of steam, and the cost of the generated electricity is 0.043 $/kWh.

http://dx.doi.org/10.5772/60207

Items	MSF-BR (TBT=110)	NF-MSF-DM (TBT=130)	% diff
Evaporator	1,066,100.45	1,570,420	47%
Pumps	306,223.35	246,014	-20%
Piping, valves, I&C	302,666.77	179,202	-41%
Intake	394,560.00	194,416	-51%
Total	2,069,550.57	2,190,052	6%
NF	-	1,339,020.42	100%
Total	2,069,550.57	3,529,072.713	71%

Table 8. CAPEX analysis of MSF and NF-MSF-DM configurations [14]

	MSF-BR	NF-MSF-DM	% diff
LP steam cost	186.23	96.9	-48%
Electricity	23.8	30.23	27%
Chemicals	0.48	0.49	2%
Total, MSF	210.92	127.63	-39%
NF		12.9	
Total, MSF-NF	210.92	140.53	-33%

Table 9. OPEX analysis of MSF and MSF-DM-NF [14]

The OPEX cost analysis (Table (9)) shows that the cost for NF-MSF-DM is 31% lower than that for the conventional MSF. The reduction in OPEX contributed to the reduction of the heating steam cost due to higher GOR. The levelized cost showed that the unit product cost of NF-MSF-DM is 21% lower than that of the conventional MSF as shown in Table (10).

As shown in Table (9), the low-pressure steam cost for the MSF-DM configuration is 48% lower than that for the conventional MSF-BR, and the steam consumption of MSF-DM is 100% lower than that consumed by the conventional MSF-BR. This is mainly due to the different steam cost invoked from the power side, as the heat steam temperature is higher in MSF-DM (TBT=130). The electricity cost of the MSF-DM is 27% higher than that of the conventional MSF-BR due to higher pumping power of the same order. The chemical cost is only 2% higher than that for the conventional MSF-BR. This is mainly due to the increase of make-up to be treated. The total number of OPEX items in the proposed configuration, MSF-DM, is 33% lower than that in the conventional MSF-BR, mainly due to low amount of steam consumption.

The annual investment cost (fixed capital cost depreciation rate (FCCDR) per year) of each component in the desalination plant is calculated according to the following relation:

$$\text{Annual Investment} = \text{CAPEX} \times \frac{i \times (1+i)^n}{(1+i)^n - 1} \tag{27}$$

Using an interest rate, i, of 7% and number of amortization years, n, of 20 years: then, the operation and maintenance cost is calculated by multiplying the equipment purchase cost by a factor of the equipment cost index. The hourly cost ($/hr) of the desalination plant is calculated as follows:

$$hourly - CAPEX = \frac{\text{Total annual investment}}{365 \times 24 \times 0.9} \tag{28}$$

Similarly, the hourly OPEX is calculated as follows:

$$hourly - OPEX = \text{LP steam} + \text{Electricity} + \text{Chemiclas} \tag{29}$$

Then the unit product cost of the desalted water is calculated as follows:

$$\text{Unit product cost, } \$/m^3 = \frac{hourly\_CAPEX + hourly\_OPEX}{hourly\_\text{Pr}oduct} \tag{30}$$

The levelized cost of capital purchased components and operating invested (chemicals, steam, electricity, O&M) to produce water is calculated as shown in Table (10). The specific OPEX of the MSF-DM is 34% lower than that of the conventional MSF-BR. The specific CAPEX of the MSF-DM is 12% higher than that of the conventional MAF-BR. However, the sum of the total cost invested using the MSF-DM is 34% lower than that of the conventional MSF-BR. Due to adding of the NF system, the specific OPEX of NF-MSF-DM is 20% lower that of the conventional one, while the specific CAPEX increased by 84% as shown Table (10). The total unit product cost of NF-MSF-DM is 9.5% lower than that of the conventional MSF-BR.

Levelization cost, $/m^3	**MSF-BR**	**NF-MSF-DM**	**% diff**
Interest rate	0.07	0.07	-
Life span	20	20	-
Amortization factor	0.094392926	0.094392926	-
Annual investment	192468.7044	215680.4949	12.06%
Hourly production	208.07	208	-0.03%
Hourly investment	24.41257032	27.35673451	12.06%
Specific CAPEX	0.117328641	0.131522762	12.10%
Specific OPEX	1.014038462	0.613605769	-39.49%
Total	1.131367102	0.745128531	-34.14%
NF			
Specific OPEX, NF	-	0.062023194	-
Specific CAPEX, NF	-	0.08493315	-
Specific CAPEX, NF-MSF-DM	0.117328641	0.216455912	84.49%
Specific CAPEX, NF-MSF-DM	1.014038462	0.807151725	-20.40%
	1.131367102	1.023607638	-9.52%

Table 10. Levelized cost of MSF and NF-MSF-DM configurations [14]

http://dx.doi.org/10.5772/60207

4.2. Hybrid FO-MSF

In this section, technical approach to consider the impact of TBT and varying FO recovery on the process performance is presented. The VDS software [18] will be used as a powerful simulation tool. In this program, a reference MSF plant of 16.2 MIGD working at TBT=111°C is simulated. The performance ratio, distillate production, concentration and flow rates, and temperatures of all streams are calculated. The software is adapted and developed to consider the FO membrane. The hybrid MSF-FO is simulated at fixed brine recycle flow rate and brine concentration (draw solution) and by varying the FO recovery ratio with the TBT. For a fixed performance ratio, the distillate of MSF (D) and the required heat transfer surface area (A) are calculated at different operating conditions. For comparison, the specific heat transfer area (SA) is calculated as:

$$SA = \frac{A}{D} \text{ m}^2/\text{MIGD} \tag{31}$$

For the same seawater and draw solution flow rate across the FO membrane, the permeate (D_m) and the membrane area (A_m) are calculated at different recovery ratios. For comparison, the specific area of FO membrane (SA) is calculated as follows:

$$SA = \frac{A_m}{D_m} \text{ m}^2/\text{MIGD} \tag{32}$$

At certain FO recovery ratio, the reduction in the Ca+ ions in the MSF feed is calculated and compared to the reference MSF process, which was operated without the FO process. The potential of $CaSO_4$ scale formation in the MSF feed after dilution is estimated at different TBTs (115-135°C) using the Skillman index.

Using VDS, all process stream characteristics are determined (mass, temperature, pressure, entropy, and rated cost), and the heat transfer surface area (number of tubes), evaporator size, internal dimensions, and pumps are sized. So, a detailed CAPEX analysis is performed and estimated. The VDS software calculates the heating steam consumption rate and the consumed chemicals (anti scales, anti-foam, and chlorination), as well as the pumping power (OPEX items). The price of electricity and heating steam is estimated and calculated as illustrated in [18]. Then the final tariff of water unit cost is obtained.

Figure 15 shows the reduction in Ca^+ ions in the feed of MSF desalination system at different recovery ratios of the FO membrane system. The reduction of Ca ions increases as the FO recovery ratio increases. At 40% recovery ratio, the reduction in Ca ions is calculated as 20%.

Figure 16 shows that the FO membrane water flux decreases as a result of the increase in the FO recovery ratio. The membrane flux decreases at higher recovery ratio due to dilution of the draw solution, which decreases the osmotic pressure driving force.

Figure 17 shows that the specific membrane area increases as the recovery ratio increases; this is due to lower water flux per unit area at higher recovery ratio. The higher value of specific membrane area is reflected in higher capital cost.

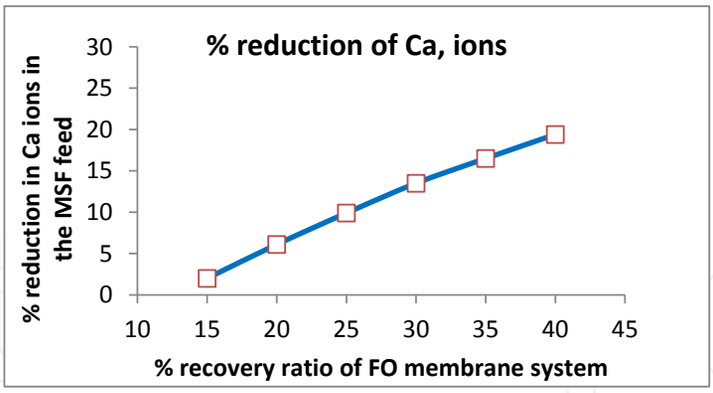

Figure 15. reduction in Ca^{+} ions in MSF feed after FO dilution

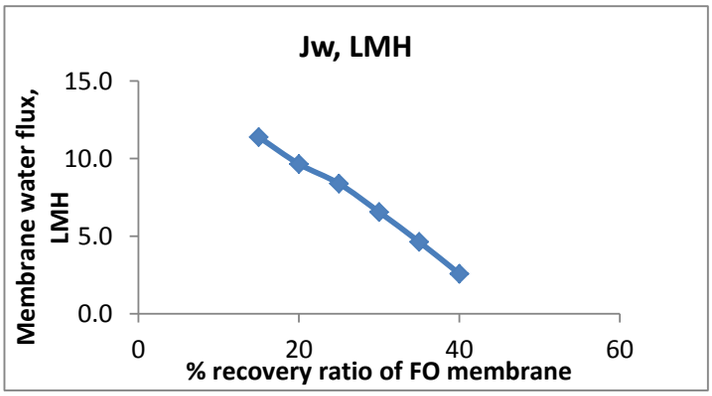

Figure 16. FO membrane flux at FO membrane recovery ratio variation

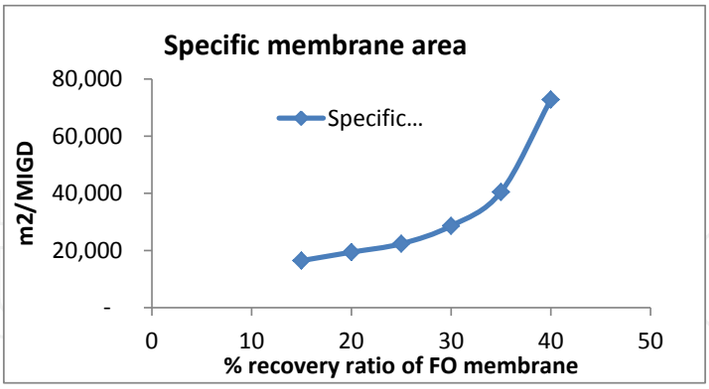

Figure 17. Membrane area variation with FO recovery ratio variation

Figure 18 shows the Skillman index (SI) at different TBTs and the variation of FO recovery ratio. The SI of calcium sulphate solubility in case of the reference MSF plant without FO operating at TBT=111°C is calculated as 1.33. As the calculated SI of traditional MSF is greater than 1, the precipitate of calcium sulphate occurs. However, in practical MSF plant anti-scalant is used to disperse the crystalized scale. The SI=1.33 is considered as the reference for comparison; the value above 1.33 indicates scale formation, while the lower value indicates safe

http://dx.doi.org/10.5772/60207

operation. As shown in Figure 5, the SI at different TBTs decreases as the FO recovery ratio increases. This is due to the increase in the removal of divalent ions. Figure 5 shows that the Skillman index increases as TBT increases. The MSF can operate at TBT=135 safely without scale problems at an FO recovery ratio of 40%. MSF at TBT=130°C can operate safely at a recovery ratio of 35%. Also, the MSF at TBT=125°C can operate safely at a recovery ratio of 30%. The MSF can operate safely at TBT=120°C and FO recovery ratio of 25%, while the MSF can operate safely at TBT=115°C and FO recovery ratio of 20%.

For the same performance ratio of MSF (PR=9), the reduction in the specific heat transfer surface area of MSF is calculated at different TBTs and different FO recovery ratios as shown in Figure 6. This figure shows that the reduction in specific heat transfer of MSF increases as the TBT increases. The increase of TBT resulting in increase of the logarithmic mean temperature difference between hot and cold streams of MSF, in turn, reduces the heat transfer area. Figure 6 shows that the reduction in SA slightly increases with the increase of the FO recovery ratio.

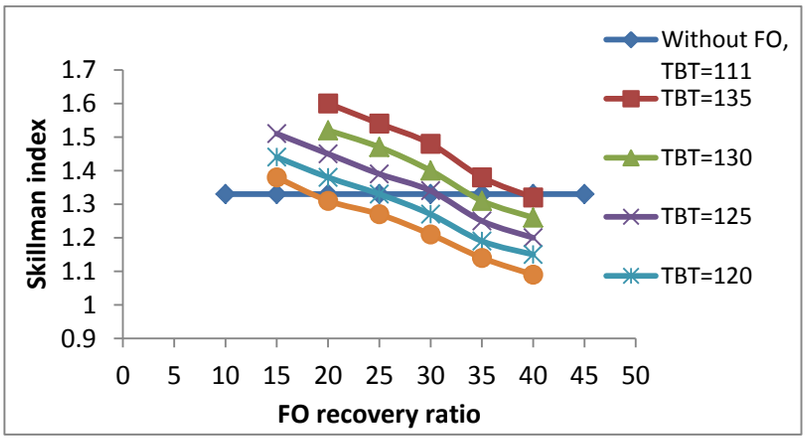

Figure 18. Skillman index at different MSF TBTs and different FO recovery ratios

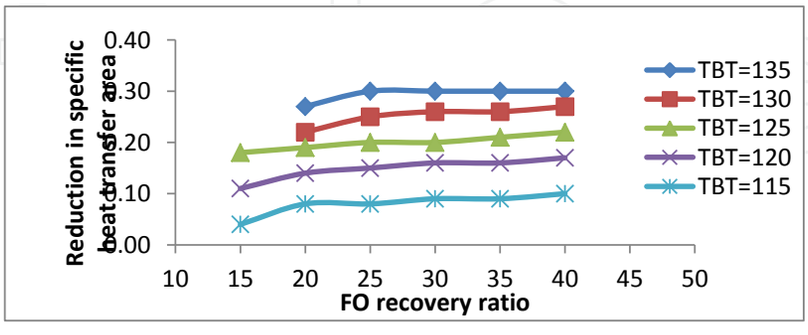

Figure 19. Reduction in the heat transfer area (CAPEX) at different FO recover ratios and TBTs

For the existing MSF plant, at TBT=130°C, the production will increase up to 30% as shown in Figure 19. The question is whether or not the existing material can withstand the 135°C temperature.

Figures 17, 18, and 19 indicate that it is beneficial to work at higher TBT to reduce the heat transfer area or to increase the production of the existing plant of MSF (CAPEX/OPEX reduction); however, this requires higher recovery ratio of the FO membrane system, which requires higher membrane area (CAPEX increase). So, an economical evaluation and compromise to reach the trade-off point is still required.

The existing capacity of water desalination plants in Qatar is approximately 1.5 Mm^3/day. MSF represent the main technology in Qatar. The make-up of seawater feed is chemically treated (anti-scalant, anti-foulant, and sodium sulphate) before being introduced to the heat recovery section. The amount of make-up flow rate is 3 times of the water production capacity, which is 4.5 Mm^3/day. As shown in Table (11), the chemical cost is 2.35 M$/year.

Chemical	Dosing rate, ppm	Consumption, kg/day	$/year
Anti-scalant	2.5	2.81E+03	2.28E+06
Anti-foam	0.1	1.35E+01	3.08E+04
Sodium sulfate	0.5	2.25E+02	4.11E+04
Total			2.35E+06

Table 11. Chemical cost analysis of thermal desalination plant

Thus, it can be concluded that the integrated FO as a pretreatment unit to the seawater feed to the existing MSF desalination plant in Qatar is technically visible in terms of production capacity increase and chemical consumption decrease. However, cost analysis is required to balance the OPEX reduction with the addition caped of the FO membrane unit. Integrating FO to the existing MSF and using the brine of the last stage as a draw solution at a recovery ratio of 35% reduce the Ca^+ ions in the seawater feed by 20%, which enables increasing the TBT up to 130°C safely. The simulation results show that at TBT=130°C, the production of the existing MSF plant increases by 20%. The OPEX analysis showed that an amount of 2.3 M$/year of chemical cost can be saved if the FO is deployed to the existing MSF plant in Qatar. The trade-off point between the additional CAPEX of the FO membrane system and the savings in OPEX will be considered under different operating condition in the present work.

5. Experimental study of hybrid NF-MSF

The process design and simulation for the test pilot is developed to prepare specifications of different components. Some units are manufactured by an Egyptian contractor, while others are purchased from vendors. The site is prepared where civil work and foundation are constructed. The test pilot components are installed and assembled, and finally, individual commissioning for each component is carried out. The site is located at the "Wadi El-Natroun" remote area, which is almost 150 km south-west of Alexandria city (Egypt). The site belongs to Alexandria University.

http://dx.doi.org/10.5772/60207

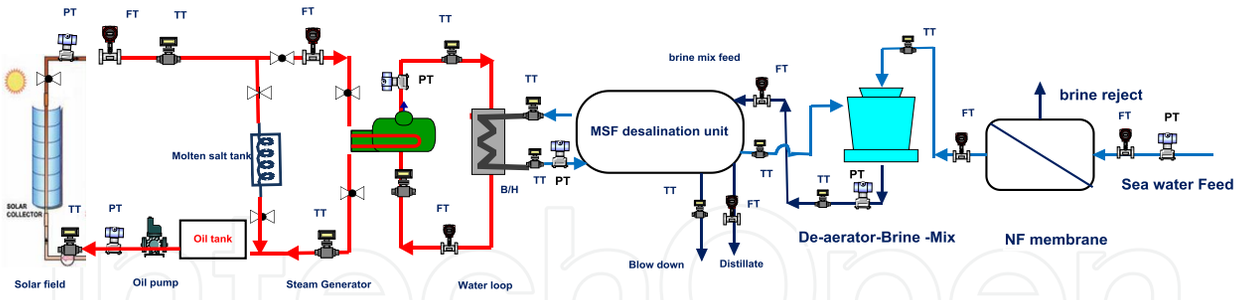

Figure 20. Basic flow diagram of CSP-NF-MSF-DBM pilot plant [13]

Figure 20 shows the pilot test of the solar energy and desalination units. The concentrated solar parabolic trough with thermal energy storage facility provides the necessary heating to generate the required steam of the MSF desalination unit. The system is also equipped with a backup boiler for steam compensation. Solar PV and wind turbine (not present in Figure 20) are installed and run separately. However, in this phase, diesel engine is used to provide the pump electricity until the match and synchronization between the PV and the wind turbine are finalized.

5.1. MSF desalination unit

The MSF pilot unit consists of 28 flashing chambers with 28 connected condensers as shown in Figures 21.a and 21.b. The stages are arranged in double deck to reduce the foot print. There are four sets; each set consists of 7 stages. MSF chambers are equipped with glass windows for monitoring of the flashing process. The shell material of MSF is fabricated from 2 mm-thick stainless steel 316L. The flash chamber is 0.5 m in length and 0.5 m in width, while the height is 1.0 m. The condenser tube is 8 mm in diameter, 6 m long, and made of stainless steel (0.7 mm thick). The number of tubes is 2 per condenser, which are arranged in multi-pass inside a 0.5 m shell length. The unit is manufactured in Egypt and assembled at the project site.

The orifice opening area is controlled using gate valve, which is located between the flash chambers. The inter-stage valves controls the inter-stage flow rates to guarantee the brine flashing at each stage. The splash plate is designed just above of the inlet opening to reduce the carry-over. A demister is placed near the vapor outlet vapor pipes to reject the brine carry-over before going to the condenser. The shells are insulated to minimize energy losses. In addition to the brine heater, different supporting systems are added including vacuum system and chemical injection systems. The vacuum system has control valves at each stage to adjust the venting rate of non-condensable gases (NCG) and the stage pressure.

The MSF is the main subsystem where distillation is produced using the flashing process. Different instrumentations are installed to measure and record the temperatures, pressures, and flow rates as shown in Figure 20. In the heating section, steam input and output temperatures, in addition to pressure and flow, are measured using proper transducers. All chambers are equipped with temperature and pressure indicators. The first and last chambers are equipped with temperature transmitter (TT) and pressure transmitter (PT), and the two

a- Double deck MSF desalination test pilot unit

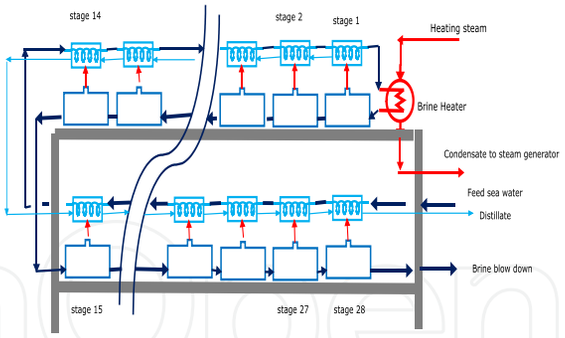

b- Process flow diagram of Double deck MSF

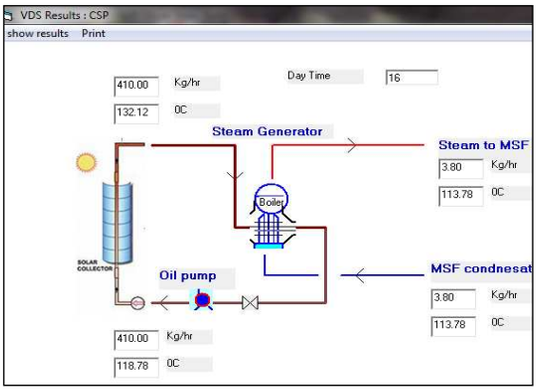

a- VDS simulation results of CSP[13]

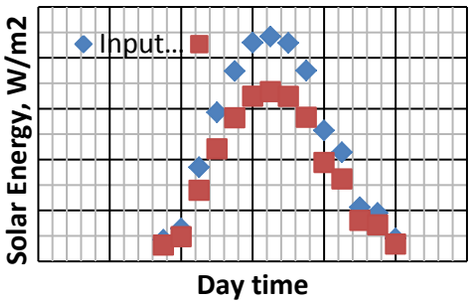

b- Solar and absorbed energy [13]

Figure 21. MSF desalination unit with double deck [13]

additional movable PT and TT are supplied to be inserted in the chambers of the operator choice. Input seawater flow and output brine and distilled water flow rates are measured using flow transmitters.

5.2. Concentrated solar power (CSP) system

Four modules of solar concentrator (parabolic trough) are purchased and assembled in series at the site of the project as shown in Figure 22. Each module is 3.6 m in length and 1.524 in width. The collector area per module is 5.6 $m^{2,}$ while the collector reflective area is 5 m^2. The assembled collector length becomes 14.6 m, while the total area is 22.4 m^2. The receiver absorptivity is 0.92, the mirror reflectivity is 0.91, while the receiver emittance is 0.23. The black-coated pipes are 1.0 inch in diameter and placed in 2.0-inch-diameter glass pipes to minimize convection losses. The concentrators have a tracking system and were placed east-west and facing south.

The CSP system contains a steam generator to supply the MSF brine heater with the required heating steam. Thermal oil is circulated through the collecting pipes, gains the solar thermal energy, and flows through the steam generator and energy storage tank. The steam generator

http://dx.doi.org/10.5772/60207

Figure 22. Four modules of the concentrated solar collector in series [13]

consists of shell and tube and has a separate vapor header. The shell diameter is 10 inches and is 2 m in length. The hot oil passes through tubes, while the water flows through the shell. The tube length is 4 m, and the diameter is 6 mm; the number of tubes is 24, which are arranged in two passes. The CSP system is instrumented with temperature transmitters (TT), flow meters (FT), and pressure transmitters (PT), as shown in Figure 20, to monitor the temperatures, flow rates, and pressure in both steam and oil loops.

5.3. NF pretreatment

Figure 23.a shows the P&I diagram of the NF system. The system consists of dual media filter, cartridge filter, high-pressure pumps, chemical injection pumps, and nano-filtration (NF) membrane. One dual media filter vessel is installed with a specified feed flow rate of 1.5 ton/hr and 3.5 ton/hr for back wash. The vessel contains sand, gravel, and anthracite. The cartridge filter of 5 micron is installed after high pressure pump and just before the membrane section. The membrane section consists of 4 pressure vessels running in parallel; each vessel contains one membrane element of NF270 4040 type. The whole NF system, except feed, permeate, and brine tanks, is placed inside one container with its control panel, as shown in Figure 23.b. For water salinity, samples are collected periodically to measure the conductivity using a mobile conductivity meter.

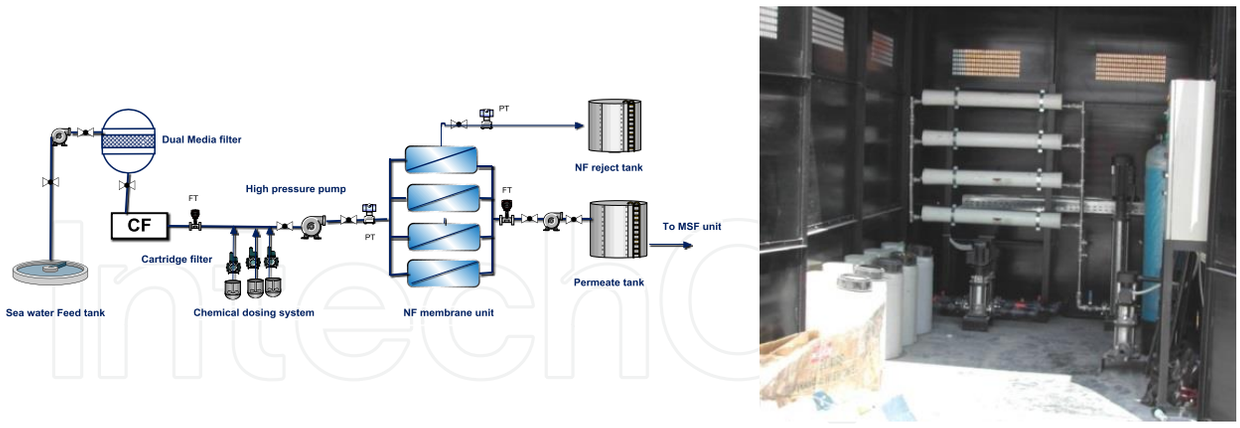

a- Process Flow Diagram of NF system

b- Photo of NF room

Figure 23. Nano-filtration (NF) system [13]

5.4. NF test performance

The NF system testing is carried out using the site brackish water (TDS=2000 ppm). A mathematical model of the NF membrane is developed and verified against typical operating NF unit data using the VDS software developed by the authors [13-15]. The VDS simulation results of the NF system were derived at different feed pressures of 8 and 10 bars and compared with experimental results as shown in Table (12). The NF performance was carried out and assessed by the recovery ratio and salt rejection. The recovery ratio (permeate/feed) increases as the feed pressure increases. The salt rejection (1- (permeate salinity/feed salinity)) is calculated as shown in Table (12). The salt rejection decreases as the feed pressure increases due to the increase in permeate salinity. The measured recovery ratio is slightly lower than the simulation results, although the salt rejection determined in the experiment is lower than that of the simulation. The differences between the measured values of permeate flow, salinity, recovery ratio, salt rejection, and simulation results are within the acceptable range.

	VDS	Exp	% diff	VDS simulation	Exp	% diff
Feed pressure, bar	8			10		
Feed flow rate, ton/hr	1.325			1.375		
Feed salinity, ppm	2000			2000		
Permeate flow rate, ton/hr	0.67	0.6	-10%	0.85	0.76	-11%
Permeate salinity, ppm	648	600	-7%	761	650	-15%
Brine flow rate, ton/hr	0.65	0.725	12%	0.52	0.6	15%
Brine salinity, ppm	3395	3158	-7%	4027	3760	-7%
Recovery ratio, %	51	45	-12%	62	55	-11%
Salt rejection, %	67.6	70	4%	62	68	10%

Table 12. Typical NF experimental results compared with the VDS results [13]

http://dx.doi.org/10.5772/60207

5.5. Concentrated solar power (CSP) test performance

The CPS system, including the solar collector and steam generator, is simulated using the VDS program. The mass and heat balance equations of the solar collector, steam generator, and pumps are developed. The oil and water thermo-physical property correlations at different temperatures are considered in the program. The characteristic surface of collector reflectivity, receiver emission and absorptivity, and glass tube material transmittance are specified in the VDS program. The specifications of the solar collector and steam generator are defined and fed to the program. The measured weather conditions (solar intensity, ambient temperature, and wind velocity) at each hour are fed to the program. The duration time starts at 7:00 AM and ends at 8:00 PM with 1 hour step.

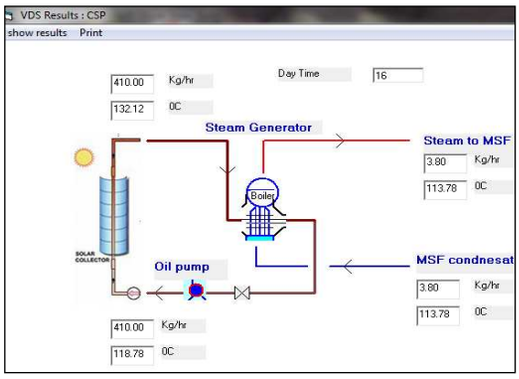

a- VDS simulation results of CSP[13]

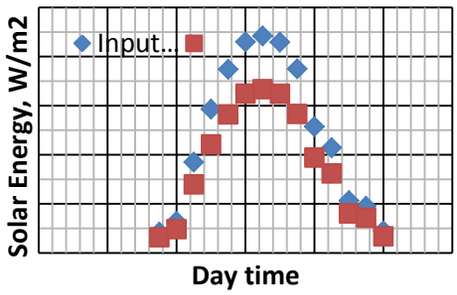

b- Solar and absorbed energy [13]

Figure 24. ADD CAPTION

Figure 24.a shows the interface of the VDS program results at 4:00 PM. The oil mass flow rate and the temperature at inlet and outlet for both the solar collector and steam generator are presented. The collected energy is transferred to the steam generator to generate 3.8 kg/hr of saturated steam at 113.8°C. The solar intensity (I) and calculated absorbed energy by the receiver are shown in Figure 24.b. The difference is noticeable at mid-day time.

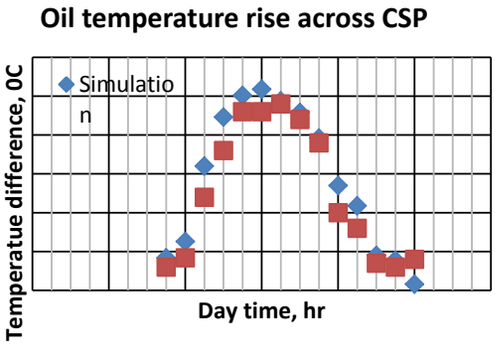

a- temperature rise in CSP

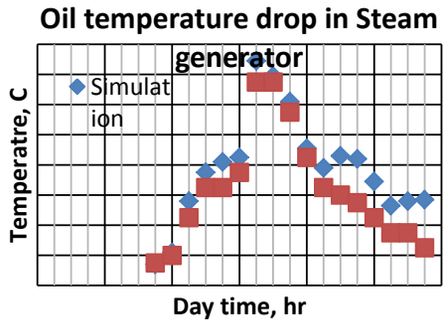

b- Temperature drop in steam generator

Figure 25. Oil temperature variation through CSP trough and steam generator [13]

Figure 25.a shows comparison between the VDS simulation and experimental results of oil temperature rise through the solar collector during day time. The oil temperature difference increases as the solar intensity increases, while the maximum difference at mid-day reached 25°C. Figure 25.b shows a comparison between the simulation and experimental results of the oil temperature drop in the steam generator unit. The maximum heat transfer occurs during mid-day, and the maximum temperature drop is 14°C. It is similarly noticed that at day time, the temperature drop in steam generator unit is less than the temperature rise in the solar collector. This means that part of the gained energy in the collector is absorbed in the steam generator, and the remaining is maintained with the outlet oil stream from the steam generator and comes back the collector. This explains the increase of oil temperature at the concentrated solar collector inlet at day time.

The CSP system average efficiency () is calculated as the average useful gained power/average solar input power:

$$\eta_{CSP} = \frac{\dot{m} C_p \Big|_{oil} (T_{o,oil} - T_{i,oil})}{I \times A_{CSP}} \tag{33}$$

Figure 26 shows the simulation and experimental results of the collector efficiency at day time. The collector efficiency decreases during day time due to the increase in the average oil temperature, which increases the energy loss to the ambient. The experimental collector efficiency shows relatively low value than that of the simulation collector efficiency due to: i) inaccurate tracking system that could not follow the sun movements accurately, and ii) the inefficient concentrated tube location in the CSP focus and possible convection loss.

Figure 27 shows comparison between the simulated and the measured generated steam temperatures. The water inlet and steam exit valve remain closed while the oil valves are open to allow energy transfer from oil to heat the enclosed water in the boiler. The water feed and steam valves are opened when the water temperature reaches 77°C. The generated steam temperature increases as the solar intensity increases, and the maximum temperature reached is 110°C at mid-day time.

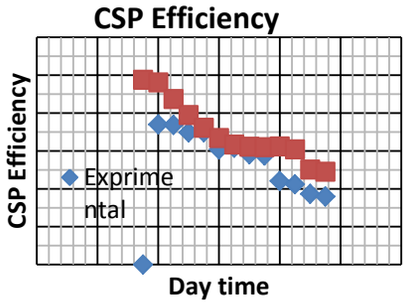

Figure 26. ADD CAPTION

http://dx.doi.org/10.5772/60207

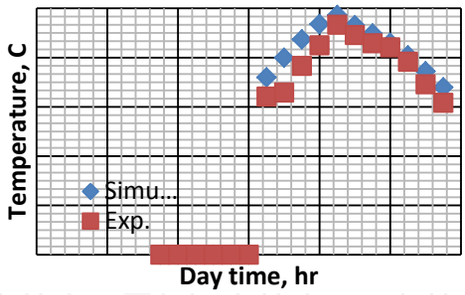

Figure 27. ADD CAPTION

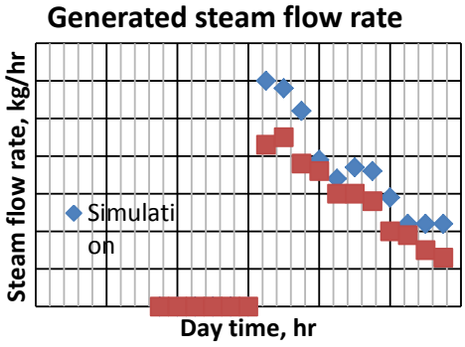

Figure 28. Generated steam flow rate [13]

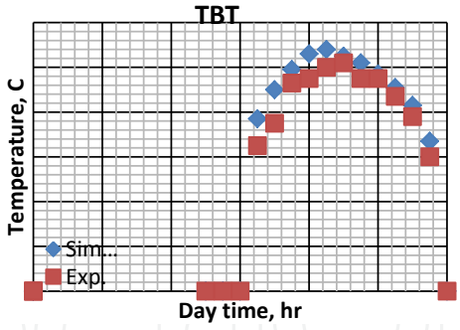

Figure 29. TBT variation [13]

The steam valve is opened at 1:00 PM at a steam flow rate of 4.3 kg/hr. The generated steam is directed to the MSF desalination unit as a heating source. The condensate steam in the brine heater of MSF is fed back to the steam generator. The amount of generated steam flow rate decreased linearly, as shown in Figure 28, due to the decrease in the solar collector efficiency. The measured generated steam flow rate shows lower values than the simulation results due to the thermal losses encountered through insufficient insulation of steam generator and throughout the connection pipe between the CSP outlet and steam generator. As shown in Figure 28, the operation of the steam generation extends up to 11:00 PM due to the heat storage in the CSP system.

Figure 29 shows the simulation and experimental values of TBT variation during day time. As the CSP steam condenses in the brine heater of MSF, the TBT rises up due to the gained energy of the latent heat. Under the ambient and operating condition in June 2012, the midday TBT reaches up to 100°C while the CSP steam condenses at 106°C, that is, 6°C temperature difference is maintained.

5.6. New MSF with de-aerator and brine mix (DBM)

The permeate water of the NF system is directed to the de-aeration and brine mix tower, where the feed is sprayed for oxygen removal. The deaerated water is mixed with parts of the brine blow down, then it is pumped to the MSF condensers. The brine mix feed absorbs latent heat energy in condensers before passing though the brine heater where the brine reaches its top temperature (TBT). The brine is then directed to the first flash chamber where flashing process occurs and vapor releases. The released vapor condenses to form product water. The flashing process occurs in the successive stages until the last stage is reached, where the un-flashed brine exits as brine blown down. The condensate of all stages is collected and directed to the water product tank. The brine level is adjusted above the interconnecting pipes (inter-stage gates) to guarantee the sealing of the flash chambers.

Under the same feed saline water flow rate (NF permeate) of 370 kg/hr and feed temperature of 27°C and controlling the brine mix ratio at 20-70% of the MSF brine blow down, the distillate water is measured and recorded at different TBTs, as shown in Figure 30, as compared with design calculated values. The pressure of saline water before the first chamber is controlled and fixed at an absolute value of 1.5 bars (above saturation conditions) by partially closing the valve. Also, the orifices among chambers are controlled by partially closing the valve between the two successive chambers. The in-tube water velocity is controlled at 2 m/s.

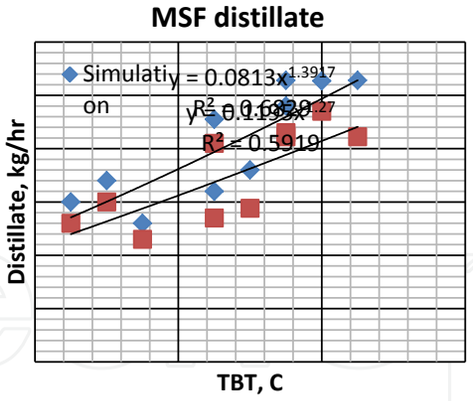

Figure 30. MSF distillate productivity with TBT variation [13]

The rates of both the design and the measured distilled water increase as a result of the TBT increases as shown in Figure 30. The amount of distillate is lower than the expected; this may be due to the partial loss of flashed vapor through vacuum system and the irreversibility of the flashing process that occurs within the orifices and weirs.

Figure 31 shows the design and the experimental GOR of the MSF variation with TBT. This is defined as the ratio between the distillate flow rate and the heating steam consumption,. The

http://dx.doi.org/10.5772/60207

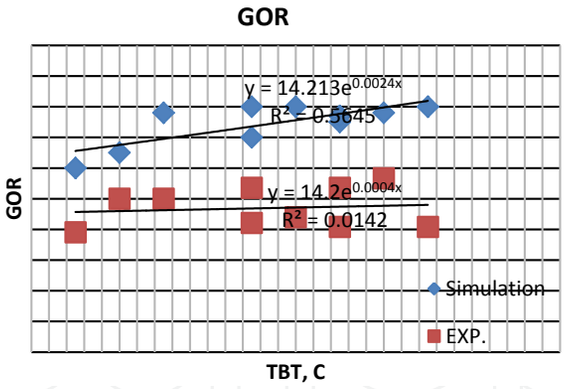

Figure 31. The GOR of MSF system variation with TBT [13]

average value of the unit design GOR is 17, which is almost twice of the conventional MSF GOR. The average measured GOR is 15 as shown in Figure 31. The small difference between the measured and designed values of GOR is due to the lower distillate productivity under fixed amount of heating steam flow rate.

The MSF specific power consumption (SPC) is defined as the ratio between the pumping power consumption (kW) and the rate of water distillate (m^3/hr),.

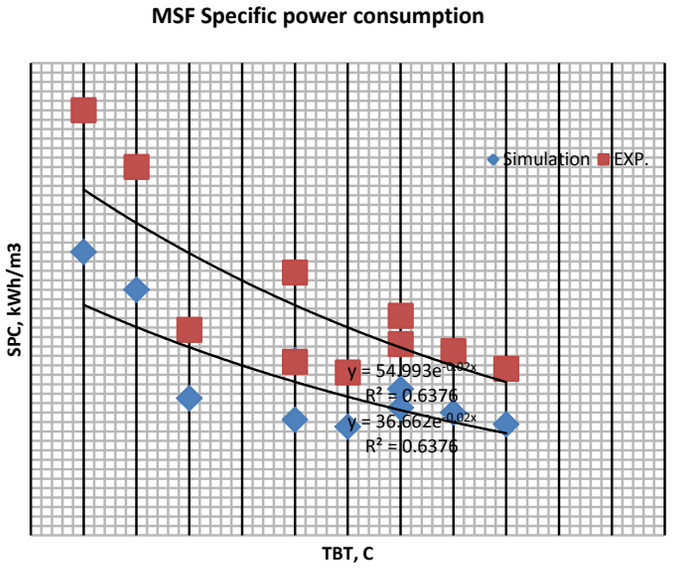

Figure 32. Specific power consumption (SPC) of MSF with TBT variation [13]

Figure 32 shows that the SPC decreases as the TBT increases mainly due to the increases in water productivity. The experimental SPC is calculated based on the measured distillate flow rate and the rated power consumption. The experimental SPC is higher, however, than the design value mainly due to lower experimental distillate for the same saline water feed and may be due to the pressure drop in piping and valves that were not considered properly in the design stage. The SPC of the test pilot unit is relatively higher than that of the commercial value of large scale MSF desalination plant due to the very small test pilot unit productivity.

6. Conclusion

To date, commercially available hybrid desalination plants are of the simple non-integrated type. They may share common systems such as intake and outfall facilities, but otherwise, they run independently at the same site. Product water from the membrane and thermal systems are usually blended to international standards on water quality. One more step ahead this chapter addresses the role of using FO or NF as a pre-treated method to the existing thermal desalination plants. The target of this hybridization is to reduce divalent ions that cause hard-scale deposition at elevated temperatures. The separation of divalent ion enables increasing the desalination process temperature greater than 110°C, which consequently increases the plant performance, increases the productivity, and reduces chemical consumption.

Integrating the NF system with new (MSF-DM) configuration at TBT=130°C, the gain output ratio could be as high as 16, which is double of that for the conventional MSF-BR. The new NF-MSFDM configuration significantly reduces the unit's input thermal energy to suit the use of (the relatively expensive) solar energy as a desalination plant driver.

Simulation results showed that integrating FO to the existing MSF and using the brine of the last stage as a draw solution at a recovery ratio of 35% reduce the Ca^{+} ions in the seawater feed by 20%, which enables increasing the TBT up to 130°C safely. The simulation results show that at TBT=130°C, the production of the existing MSF plant increases by 20%. The OPEX analysis showed that an amount of 2.3 M$/year of chemical cost can be saved if the FO is deployed to the existing MSF plant in Qatar.

The desalination pilot test is built to evaluate the performance of the novel de-aeration and brine mix (MSF-DBM) configuration at high TBT using the NF membrane. The capacity of the desalination pilot plant is 1.0 m^3/day of water. Comparison between the simulation and the experimental results of the pilot unit subsystems is relatively satisfactory. The newly developed NF-MSF-DBM (de-aerator and brine mix) configuration is tested at TBT=100°C, and the GOR is calculated as 15, which is almost twice of the traditional MSF under the same operating conditions. Using the new high-performance NF-MSF-DBM and the unit's input thermal energy, which make the integration with (the relatively expensive) RE as a desalination plant driver, is a viable option.

Author details

Abdel Nasser Mabrouk[1,2*], Hassan Fath[3], Mohamed Darwish[1] and Hassan Abdulrahim[1]

*Address all correspondence to: aaboukhlewa@qf.org.qa abdelnaser.mabrouk@suezuniv.edu.eg

1 Qatar Environmental & Energy Research Institute, Qatar

2 Suez University, Egypt

3 American University, Sharjah, UAE

http://dx.doi.org/10.5772/60207

References

[1] K.P. Jong. Application of hybrid technology to the largest desalination plant, Fujairah, UAE, IDA World Congress, Bahamas (2003).

[2] H. Ludwig. Hybrid systems in seawater desalination, Desalination, 164 (2004) 1.

[3] Ata M. Hassan. Process for desalination of saline water especially water, having increased product yield and quality, Patent No. US 6,508,936 B1.

[4] Hassan Ata. Fully integrated NF-thermal seawater desalination, process and equipment, US Patents No 2006/0157410 A1, July 20, 2006.

[5] M. Al Sofi, Atta Hassan, G. Mustafa, A. Dalvi, N. Kithar. Nanofiltration as means of achieving higher TBT of >120 C in MSF, Desalination 118 (1998) 123–129.

[6] Atta Hassan, A. Al Sofi, A. Al-Amoudi, A. Jamaluddin, A. Farooque, A. Rowaili, N. Dalvi, G. M Kithar, I. Al-Tisan. A new approach to membrane and thermal seawater desalination processes using nanofilteration membranes (Part I), Desalination 118 (1998) 35–51.

[7] L. Awerbuch. Water desalination process using ion selective membranes, US Patent, No. 2005/0011832 A1, January 20, 2005.

[8] O. Hamed, A. Hassan, K Al-Shail, K. Bamardouf, S. Al-Sulami, Ali Hamza, M. Farooque, A. Al-Rubaian. Higher TBT, more product, less scaling, Desalin, Water Reuse 13/3, IDA, November/December (2003).

[9] S. May. Hybrid desalination systems, Middle East Desalination Research Center (MEDRC) Report (2000).

[10] O. Hamed. Overview of hybrid desalination systems, Desalination, 186 (2005) 207.

[11] Al-Mulla. Integrating hybrid systems with existing thermal desalination plants, Desalination, 174 (2005).

[12] P.K. Eriksson. Evaluation of nanofiltration as pretreatment to reverse osmosis in seawater desalination, IDA World Congress, Singapore (2005).

[13] Abdel Nasser Mabrouk and Hassan El-banna Fath. Experimental study of high performance hybrid NF-MSF desalination pilot test unit driven by renewable energy, Desalination and Water Treatment, 2103, DOI:10.1080/19443994.2013.773860.

[14] Abdel Nasser Mabrouk and Hassan El-banna Fath. Techno-economic analysis of hybrid high performance MSF desalination plant with NF membrane. Desalination and Water Treatment, 1944-3994/1944-3986@2012, http://dx.doi.org/10.1080/19443994.2012.714893.

[15] O. A. Hamed. Development of trihybrid NF/RO/MED desalination systems, Gulf water conference, Riyadh, 2007.

[16] S. Adham, R.C. Cheng, D.X. Vuong, K.L. Wattier. Long Beach's dual-stage NF beats single stage SWRO, Desalination and Water Reuse, 13 (2003), 18.

[17] Ali Altaee, Abdel Nasser Mabrouk, Karim Borouni. A novel forward osmosis membrane pretreatment of seawater for thermal desalination processes. Desalination, 326, 19–26, October (2013). http://dx.doi.org/10/1016/j.desal.2013.07.008. (ISSN: 00119164).

[18] Ali Altaee, Abdel Nasser Mabrouk, Karim Borouni. Forward osmosis pretreatment of seawater to thermal desalination: High temperature FO-MSF/MED Hybrid System. Desalination, 339, (2014), 18-25. http://ex.doi/10.1016/j.desal.2014.02.006. (ISSN: 00119164).

[19] E. El-Sayed, M. Abdeljawad, S. Ebrahim, A. Al Saffar. Performance evaluation of two membrane configurations in a MSF/RO hybrid system, Desalination, 128 (2000) 231.

[20] Atta Hassan, M. Al Sofi, A. Al-Amoudi, A. Jamaluddin, A. Farooque, A. Rowaili, A. Dalvi, N. Kithar, G. Mustafa, I Al-Tisan. A new approach to membrane and thermal seawater desalination processes using nanofilteration membranes (Part I), Desalination, 118, 35–51 (1998).

[21] A. A. Mabrouk, A. S. Nafey, H. E. S. Fath. Thermoeconomic analysis of some existing desalination processes, Desalination, 205 (2007), 354–373. DOI: 10.1016/j.desal. 2006.02.059, (ISSN: 00119164).

[22] A. A. Mabrouk, A. S. Nafey, H. E. S. Fath. Analysis of a new design of multi stage flash-mechanical vapor compression (MSF-MVC) desalination process, Desalination 204 (2007), 482–500. DOI: 10.1016/j.desal.2006.02.046, (ISSN: 00119164).

[23] A. S. Nafey, H. E. S. Fath, A. A. Mabrouk. Thermoeconomic investigation of multi effect evaporation (MEE) and hybrid multi effect evaporation-multi stage flash (MEE-MSF) systems, Desalination, 201 (2006), 241–254. DOI: 10.1016/j.desal.2005.09.044, (ISSN: 00119164).

[24] A. S. Nafey, H. E. S. Fath, A. A. Mabrouk. Exergy and thermoeconomic evaluation of MSF process using a new visual package, Desalination, 201 (2006), 224 –240. DOI: 10.1016/j.desal.2005.09.043, (ISSN: 00119164).

[25] A. S. Nafey, H. E. S. Fath, A. A. Mabrouk. A new visual package for design and simulation of desalination processes, Desalination, 194 (2006), 281–296. DOI: 10.1016/ j.desal.2005.09.032, (ISSN: 00119164).

[26] Da Hee Jung, Jijung Lee, Do Yeon Kim, Young Geun Lee, Minkyu Park, Sangho Lee, Dae Ryook Yang, Joon Ha Kim. Simulation of forward osmosis membrane process: Effect of membrane orientation and flow direction of feed and draw solutions, Desalination, 277 (2011), 83–91.

[27] Tiraferri A., N. Yip, A. Straub, S. Castrillon. A method for the simultaneous determination of transport and structural parameters of forward osmosis membranes, J. of Membrane Science, 444 (2013), 523–538.

http://dx.doi.org/10.5772/60207

[28] M.A. Darwish, M.M. El-Refaee, M. Abdel-Jawad. Developments in the multi-stage flash desalting system, Desalination, 100 (1995), 35–64.

[29] Aiman E. Al-Rawajfeh, Hassan E.S. Fath, A.A. Mabrouk. Integrated salts precipitation and nano-filtration as pretreatment of multistage flash desalination system, Heat Transf. Eng., 33 (3) (2011), 272–279.

[30] Ata Hassan. Fully integrated NF-thermal seawater desalination process and equipment, US Patent No. 2006/0157410 A1, July 20, 2006.

[31] M. Al Sofi, Atta Hassan, G. Mustafa, A. Dalvi, N. Kithar. Nanofiltration as means of achieving higher TBT of >120°C in MSF, Desalination, 118 (1998), 123–129.

[32] Atta Hassan, A. Al Sofi, A. Al-Amoudi, A. Jamaluddin, A. Farooque, A. Rowaili, N. Dalvi, G. M. Kithar, I. Al- Tisan. A new approach to membrane and thermal seawater desalination processes using nanofilteration membranes (Part I), Desalination, 118 (1998), 35–51.

[33] X. Wang, T. Tsuru, M. Togoh, S. Nakao, S. Kimura. Evaluation of pore structure and electrical properties of nano filtration membranes. J. Chem. Eng. Jpn, (1995), 186–192.

IntechOpen